LBL-3746
c. 1

SIMPLE AND COMPLEX FLUORIDES OF GOLD AND PALLADIUM

Kevin Michael Leary
(Ph. D. thesis)

May 1975

Prepared for the U. S. Energy Research and
Development Administration under Contract W-7405-ENG-48

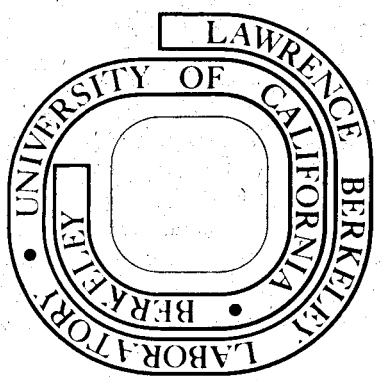

LBL-3746
c. 1

DISCLAIMER

SIMPLE AND COMPLEX FLUORIDES OF GOLD AND PALLADIUM

Contents

SIMPLE AND COMPLEX FLUORIDES OF GOLD AND PALLADIUM

Kevin Michael Leary

Inorganic Materials Research Division, Lawrence Berkeley Laboratory
and Department of Chemistry; University of California,
Berkeley, California 94720

ABSTRACT

Several compounds containing the novel AuF_6^- ion (Au(V)) were prepared and characterized using a variety of techniques. The chemistry of several AuF_6^- salts is described; the AuF_6^- ion was found to be a powerful oxidizer, oxidizing IF_5 to IF_6^+ at room temperature. The X-ray crystal structure of the salt $Xe_2F_{11}^+AuF_6^-$ was determined; the geometry of both the cation and the anion are described for the first time. The $Xe_2F_{11}^+$ ion consists of two XeF_5^+ groups bridged by a fluoride ion; the anion was found to be nearly octahedral with an average Au-F bond length of 1.86Å. A Mössbauer study of several AuF_6^- salts is reported. The values obtained for isomer shift and quadrupole splitting confirm the octahedral geometry of the AuF_6^- ion and the +5 oxidation state of gold. The bonding in gold fluorides is discussed.

Two new adducts of XeF_6 with PdF_4, $4XeF_6 \cdot PdF_4$ and $2XeF_6 \cdot PdF_4$, were prepared and characterized using vibrational spectroscopic and X-ray diffraction techniques. These compounds were shown to be $(Xe_2F_{11}^+)_2PdF_6^=$ and $(XeF_5^+)_2\ PdF_6^=$. The X-ray single crystal structure of $(XeF_5^+)_2\ PdF_6^=$ is reported. It describes for the first time the geometry of the XeF_5^+ ion in a doubly-charged anion environment.

I. INTRODUCTION

This thesis has two major divisions, Chapters II and III dealing with the attempted synthesis of Palladium(V) compounds and Chapters IV through VI dealing with the preparation, characterization and some chemistry of Gold(V) compounds.

Chapter I describes the apparatus and techniques common to most of the work in this thesis, and to inorganic fluorine chemistry in general. Specialized equipment and methods developed for particular problems are described in detail in the appropriate chapters.

A. Apparatus and Techniques

Most of the compounds described in this thesis are both extremely moisture sensitive and corrosive, so that their manipulation requires the rigorous maintenance of a dry environment. Hence, nearly all experiments required the use of a metal vacuum line and/or an inert atmosphere box. The methods and materials for handling air-sensitive compounds have been described in detail by Shriver.[1]

Vacuum lines were constructed of Autoclave Engineers 30VM6071 Monel valves (rated to 30,000 psi) and the appropriate connectors. Normal working pressures were measured with Helicoid gauges--one for the 0-1500 mm Hg range, and another for the 0-500 psia range. Pressures less than 1 mm Hg were measured with thermocouple and ion gauges which could be isolated from the system to avoid damage from corrosive chemicals. The vacuum system was equipped with three separate pumps--a small mechanical pump for the disposal of waste fluorine through a soda lime tower, a good quality mechanical pump for general work, and a 2 in. oil diffusion pump for high vacuum applications.

For general synthetic work reaction vessels and small systems constructed of Kel-F, Teflon-FEP, quartz and pyrex glass and equipped with Whitey IKS4 brass valves (Kel-F tipped stems) were used. Quartz and pyrex apparatus was connected to the system using either graded seals and/or Kovar seals, or directly using bored out Swagelok unions (e.g., 10 mm glass was used with a nominal 3/8 in. union). Teflon ferrules were stretched over the glass tubing using gentle heat from a heat gun.

For high pressure and/or high temperature syntheses, reactions were carried out in autoclave bombs fabricated of Monel/stainless steel, with thick copper gaskets, capable of withstanding 500 atmospheres pressure at 600°C. These bombs were used with nickel liners to minimize corrosion and to facilitate handling the product in the drybox.

All apparatus was carefully leak tested with a CEC 24-120B helium mass spectrometer leak detector when first assembled, and retested when connections were made or broken.

Solids (and some liquids, e.g., SbF_5) were handled in a VAC inert atmosphere box (N_2 atmosphere) equipped with two circulating drying trains that removed both water and oxygen. These were regenerated on a regular schedule (every three to four weeks) to insure the driest conditions inside the box. The gloves were inspected frequently and were replaced when they become worn or cracked.

B. Routine Characterization of Materials

1. Raman Spectroscopy

Routine Raman spectra were obtained on a Cary 83 Raman Spectrometer (488 nm). For higher resolution work, and for compounds that were sensitive to blue light, the Raman spectrometer at the USDA Western Regional Research Laboratories, Albany, California was used. This instrument provided for excitation with a variety of laser lines (principally 488, 514.5 and 647.1 nm), a Spex 1401 double monochromator, and a detection system that utilized photon counting techniques. The spectrometer was coupled to an on-line computer which allowed the data to be collected, stored, corrected for phototube sensitivity, normalized and plotted. Powdered samples were loaded into 1 mm o.d. quartz capillaries in the drybox, sealed temporarily with a plug of Kel-F grease, and the tube drawn down and sealed in a small flame outside the drybox.

2. Infrared Spectroscopy

Infrared spectra were routinely obtained on a Perkin-Elmer 337 Grating Spectrometer over the range 400-4000 cm^{-1}. A 10 cm path length Monel cell with AgCl windows (1 mm thick) was used for gases. Spectra of solids were obtained as fine powders pressed between AgCl plates in a Kel-F holder.

3. X-Ray Powder Photography

X-ray powder diffraction patterns of solid samples were obtained with a General Electric Precision camera (Straumanis loading, graphite monochromatized CuK_α radiation). Finely powdered samples were sealed into 0.3-0.5 mm quartz capillaries as described under Raman spectroscopy.

Films were measured on a Norelco measuring device.

4. Xenon Analyses

Xenon was determined using a Dumas nitrometer. Samples were loaded in the Drilab into previously dried and weighed thin-walled pyrex capillary tubes, which were then sealed as described under Raman spectroscopy. The capillaries were cleaned of grease, reweighed, and then inserted into the combustion tube of the nitrometer. The evolved gas was collected over 50% KOH solution previously saturated with xenon. Samples of XeF_2 were run to check the accuracy of the method. The nitrogen from the Drilab present in the capillaries had a negligible effect on the results.

II. ATTEMPTED SYNTHESES OF PALLADIUM(V) COMPOUNDS: THE SALTS $(XeF_5^+)_2PdF_6^=$ and $(Xe_2F_{11}^+)_2PdF_6^=$

A. Introduction

Although the hexafluorides of both rhodium and platinum are known, the highest known oxidation state of palladium is four, found in the tetrafluoride,[2] several hexahalogeno dianions[3] and the nitrate.[4] The possibility of synthesizing a Pd(V) fluoride seemed very likely, given the correct choice of experimental conditions. The synthetic approach was based on the the supposition that the electronegativity of Pd(V) in a complex anion would be less than in the free pentafluoride itself. The combination of XeF_6 and F_2 was chosen as the oxidizing system for two reasons: XeF_6 is an excellent base which is oxidatively inert.[5] The liquid was also judged likely to be a polar solvent because of the ionization of XeF_6 in the solid state.[6]

B. Experimental

Palladium Sponge was supplied by Engelhard Industries and was specified to be 99.99% pure.

BrF_3, F_2 and Anhydrous HF was supplied in cylinders by the Matheson Company.

Xenon Difluoride was prepared using the method of Streng and Streng,[7] and Holloway,[8] as given by Williamson.[9] It was characterized by its Raman spectrum.

Xenon Hexafluoride was prepared using the method of Sheft, Spittler and Martin.[10] It was characterized by its infrared spectrum.

Palladium Dibromide was obtained by dissolving Pd sponge in aqua regia then evaporating to dryness several times with a mixture of HBr and Br_2.

"Palladium Trifluoride" ($Pd^{+2}PdF_6^{-2}$) was prepared using Sharpe's method.[11]

Palladium Tetrafluoride was prepared using the method of Bartlett and Roo.[2] Material prepared in this way occasionally contained a trace of "PdF_3".

$(NO)_2PdF_6$ was prepared by dissolving NOCl and $PdBr_2$ in BrF_3 in a quartz bulb. This compound is a bright yellow solid. The Raman spectrum of $(NO)_2PdF_6$ is shown in Fig. 1, and the data is tabulated in Chapter V.

1. $4XeF_6 \cdot PdF_4$

Typically, 0.40 g Pd_2F_6 (1.22 mmoles) and 0.70 g XeF_2 (16.0 mmoles) were placed in 45 ml autoclave bomb. Then 58 mmoles of F_2 were condensed in, and the bomb was heated to 360°C for 24 hr (P = 1000 psi). It was slowly cooled to room temperature, then the excess XeF_6 and F_2 were removed under vacuum. The product, a yellow solid, was found as long needle crystals adhering to the top and sides of the bomb. Analysis for xenon gave the following: found; 43.9%, required for $4XeF_6 \cdot PdF_4$; 45.1% Xe. This material could also be prepared by substituting PdF_4 for PdF_3 in the above preparation.

2. Properties of $4XeF_6 \cdot PdF_4$

The Raman spectrum of this material is shown in Fig. 1. Caution had to be exercised in obtaining Raman spectra of these compounds; the 4:1 was photolyzed to the 2:1 by green laser light (514.5 nm) but remained stable to decomposition in red light (647.1 nm) $4XeF_6 \cdot PdF_4$ reacts explosively with water, liberating ozone smelling gases. X-ray

powder photographs gave a complex pattern, and Weissenberg and precession photographs established that $4XeF_6 \cdot PdF_4$ is triclinic,

a = 17.64(4)	α = 91.1(1)
b = 9.59(3)	β = 90.3(1)
c = 5.72(2)	γ = 99.0(1)

V = 955.5Å^3, Z = 2, space group B1 or B$\bar{1}$ (a non-standard centered cell of P1 or P$\bar{1}$).

3. $\underline{2XeF_6 \cdot PdF_4}$

The 2:1 compound can be prepared by heating the 4:1 to 50°C under dynamic vacuum; alternatively, the 2:1 can be prepared by heating the 4:1 to 400°C in a bomb under 1000 psi F_2, then cooling slowly to room temperature, excess F_2 and XeF_6 being removed under vacuum. This method yielded good-quality single crystals, several of which were used in the X-ray crystal structure determination of this compound. Analysis for xenon gave the following: found 39.3%, required for $2XeF_6 \cdot PdF_4$: 39.0% Xe.

4. $\underline{\text{Properties of } 2XeF_6 \cdot PdF_4}$

This compound is also a yellow solid which reacts violently with water. The Raman spectrum of $2XeF_6 \cdot PdF_4$ is also shown in Fig. 1. Weissenberg photographs showed that the 2:1 compound is orthorhombic,

a = 9.346(6)
b = 12.786(7)
c = 9.397(6)

V = 1122.9Å^3, Z = 4, space group $Pca2_1$ (#29).or Pcam (#57). (See Chapter III for the description of the X-ray single-crystal structure of $2XeF_6 \cdot PdF_5$.)

5. Reaction of XeF_6 with PdF_4

A PdF_4-PdF_3 mixture (0.50g, ~10% PdF_3) was placed in a Kel-F trap. XeF_6 was then distilled in, and the trap heated to 60°C for 30 min. An orange solution over a purple solid was obtained. The excess XeF_6 was removed under vacuum. This experiment yielded fairly pure PdF_4, containing only a trace of PdF_3, as shown by X-ray powder photographs. No evidence for either $4XeF_6 \cdot PdF_4$ or $2XeF_6 \cdot PdF_4$ was found in the product.

6. Reaction of XeF_6 and HF with PdF_3

PdF_3 (0.18g) was placed in a Kel-F trap. XeF_6 was distilled on to it and the mixture was heated overnight to 60°C. There was no evidence of reaction. A small amount (~1 ml) of anhydrous HF was then distilled into the trap which was shaken at intervals for 2 hr at room temperature. Only part of the PdF_3 dissolved. The XeF_6 and HF were then removed under vacuum, leaving a chocolate brown solid. A X-ray powder pattern of this material was identical to that of $4XeF_6 \cdot PdF_4$. No lines due to PdF_3 or PdF_4 were present on the film.

C. Results and Discussion

The results firmly establish the existence of 4:1 and 2:1 complexes of XeF_6 with PdF_4. Both the single crystal data (see following chapter) and the Raman spectra of these compounds indicate that they may be correctly formulated as $(Xe_2F_{11}^+)_2PdF_6^=$ and $(XeF_5^+)_2PdF_6^=$. The vibrational spectra will be discussed along with those of other $Xe_2F_{11}^+MF_6^-$ and $XeF_5^+MF_6^-$ salts in Chapter V.

It is surprising that the reaction of neat XeF_6 and PdF_4 will not yield either of the two complex salts directly. It is also somewhat surprising that XeF_6 will not oxidize PdF_3 to PdF_4 without the help of HF. However, PdF_3 is known to be very resistant to further oxidative attack.[2] Presumably, the HF aids in the oxidation of PdF_3 by XeF_6 by helping to solvate both the PdF_3 and the XeF_6, e.g.,

$$XeF_6 + HF \rightleftharpoons XeF_5^+ + HF_2^- \quad .$$

The fact that material prepared this way is brown rather than yellow may be due to the formation of a species containing polymeric palladium(IV) fluoro-anions which are amorphous to X-rays. Zemva and Bartlett have obtained evidence for these types of compounds using both XeF_6 and XeF_2 in combination with PdF_3 and PdF_4.[12] Presumably, a greater quantity of HF and or a larger concentration of the base, XeF_6, might have yielded purer material.

$PdF_6^=$ salts ($d_{t_{2g}}^6$ electron configuration) are relatively easy to prepare, but even under forceful fluorinating conditions (400°C, 1000 psi F_2) no evidence for a Pd(V), as PdF_6^-, (a $d_{t_{2g}}^5$ species) was found. However, Falconer, et al.[13] have since reported the compound $O_2^+PdF_6^-$, prepared by oxyfluorination of palladium powder at 320° and 60,000 psi. Perhaps O_2F, being a weaker base than XeF_6, does not form complexes with the lower oxidation states, but does stabilize the higher oxidation states by complex formation. XeF_6, on the other hand, forms stable complexes with Pd(IV) species. The $d_{t_{2g}}^6$ electron configuration of Pd(IV) in $PdF_6^=$ will certainly confer kinetic stability to that species and this may be a major factor in the resistance to oxidation shown by the XeF_5^+ and $Xe_2F_{11}^+$ salts.

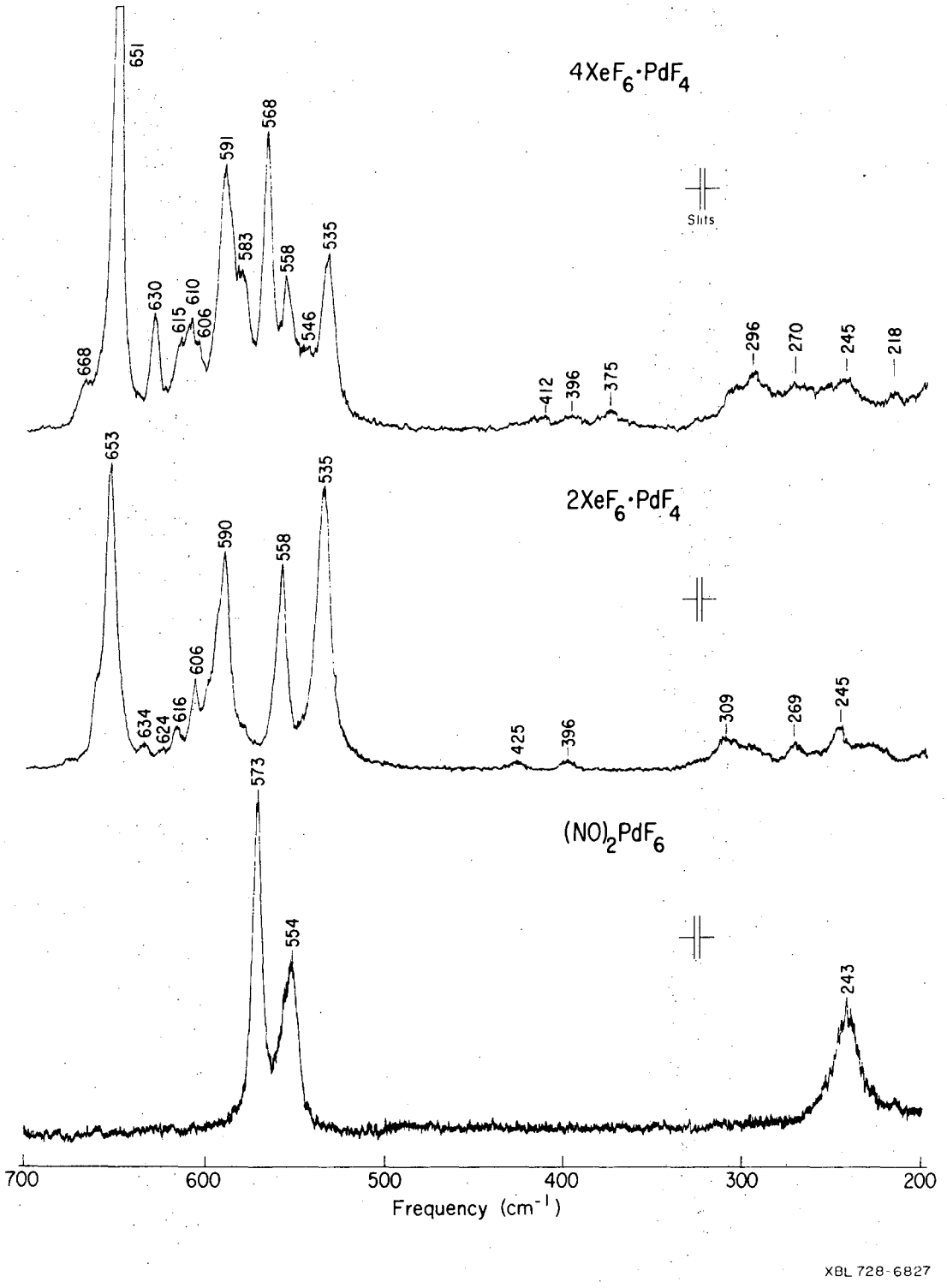

Fig. 1. Raman spectra of some $PdF_6^=$ salts.

III. THE CRYSTAL STRUCTURE OF $(XeF_5^+)_2\ PdF_6^=$

A. Introduction

The Raman vibrational data for $4XeF_6 \cdot PdF_4$ and $2XeF_6 \cdot PdF_4$ (Chapters II and V) indicated that the adducts were $(Xe_2F_{11}^+)_2\ PdF_6^=$ and $(XeF_5^+)_2\ PdF_6^=$, respectively. Because the $Xe_2F_{11}^+$ cation had not been characterized crystallographically, a full structural investigation was desirable. Crystals of the 2:1 compound were obtained during attempts to grow crystals of the 4:1; crystals of $4XeF_6 \cdot PdF_4$ satisfactory for a structural analysis were never found. Although the XeF_5^+ cation was well characterized,[5,14,15] the structure determination of the 2:1 was undertaken in order to evaluate the effect of a doubly charged anion on the geometry of the cation.

B. Experimental

1. Preparation

Crystals of $2XeF_6 \cdot PdF_4$ were prepared as described in Chapter II. Suitable sized specimens of the yellow, needle-shaped crystals were loaded into 0.2 mm o.d. quartz capillaries which had been drawn down to smaller diameter at the sealed end. Crystals were wedged into the drawn-down ends with the aid of pyrex glass push rods.

2. Crystal Data

The crystal chosen for data collection was a yellow needle with dimensions 0.3×0.2×0.1 mm. Weissenberg photographs showed $F_{16}PdXe_2$ (m.w. 673.0) to be orthorhombic, with $\underline{a}$ = 9.346(6), $\underline{b}$ = 12.786(7), $\underline{c}$ = 9.397(6)Å, $\underline{V}$ = 1122.9Å^3, $\underline{z}$ = 4 and $\underline{D}_c$ = 3.91 gcm^{-3}. The unit cell volume satisfies Zachariasen's criterion[16] for close packed fluoride lattices, the effective volume per fluorine atom being 17.6Å^3. The

systematic absences, $0k\ell$, $\ell = 2n + 1$ and $h0\ell$, $h = 2n + 1$, indicated the space group[17] to be either $Pca2_1$ (No. 29) or $Pcam$ (No. 57).

3. X-Ray Measurements

Diffraction data were collected at room temperature ($T = 24.5 \pm 1.5°$) on a Picker automatic four circle diffractometer using Mo $K\alpha$ radiation ($\lambda = 0.7107$Å). Accurate cell dimensions were obtained by measuring the 2θ angle for the Mo $K\alpha_1$ peak for the highest angle reflection observable along each of the principal axes. The c axis was oriented along ϕ.

Intensity data were collected and treated as previously described.[18] No absorption correction was applied (the absorption coefficient $\mu = 78.7$ cm^{-1}). Hence, the values for the anisotropic thermal parameters may not properly represent the thermal motion. The only other difference from the previously described procedure for the data treatment[8] was in the choice for the value of q, on arbitrary factor employed to prevent the relative errors for large counts becoming unrealistically small. A value $q = 0.04$ was assumed here. Three standards were checked over 200 reflections; their intensities increased slightly over the period of data collection.

Scattering factors for neutral F, Xe and Pd were taken from Doyle and Turner[19] and Cromer and Waber.[20] Cromer and Liberman's values[21] of $\Delta f'$ and $\Delta f''$ were used for anomalous dispersion corrections.

A complete set of $hk\ell$ and $hk\bar{\ell}$ data were collected for $2\theta \leq 45°$ (1464 unique reflections). In the least-squares refinements 1410 data which satisfied the condition $I \geq 3\sigma(I)$ were given nonzero weight.

4. Structure Refinement

At the outset, it was assumed that the structure would be centric, so the two acentric data sets were averaged to give a single data set. A three dimensional Patterson synthesis revealed the positions of two of the three heavy atoms, but it also indicated that the non-centric group ($Pca2_1$, No. 29) was appropriate. Full matrix least-squares[22] and a subsequent Fourier synthesis yielded the positions of the third heavy atom and several of the fluorine atoms. The refinement proceeded routinely down to R = 7.5% with all 19 atoms placed and the heavy atoms assigned anisotropic thermal parameters. At this point, the structure seemed to have settled into a false minimum, since bond lengths and angles gave very poor agreement with previous structures of this type. After much experimentation involving location of atoms across symmetry elements (and pseudo-symmetry elements), to generate a chemically acceptable arrangement, the R value dropped to 6.0%. Subsequent least-squares refinement with all atoms anisotropic, but using the data appropriate for the centric space group, yielded an R value of 2.0%. The data were reordered to satisfy the noncentric symmetry and to take advantage of anomalous dispersion. Two polarities or chiralities must be considered. Least-squares refinement yielded R = 0.0256 (including zero weight data), R = 0.0237 (excluding zero weight data) for the first choice with mostly positive z coordinates. For the mirror image structure least-squares refinement yielded R = 0.0260 (including zero weight data), and R = 0.0241 (excluding zero weight data). The magnitudes of the z parameters of the two forms did not differ by more than one standard deviation. The first choice was taken as correct

and is described here. A final difference Fourier showed that the largest residual electron density was -1.7 e/Å^3. The standard deviation of an observation of unit weight was 0.994. The largest shift of any parameter, divided by the estimated standard deviation on the last cycle was less than 0.003. Table I gives the final positional and thermal parameters for this refinement. The F_o, standard deviations, and ΔF data are given in Table II.

C. Description of the Structure

The asymmetric structural unit contains two crystallographically distinct XeF_5 groups and a PdF_6 group. The structural unit is illustrated in Fig. 1.

The PdF_6 group is almost octahedral. As may be seen from Table III, only one Pd-F [Pd-F(2) = 1.860(6)Å] departs significantly from the average Pd-F distance of 1.893Å. All cis F-Pd-F angles are within 5° of 90°.

The two XeF_5 groups are similar, each being an approximately C_{4v} symmetry species, with an F_{axial}-Xe-$F_{equatorial}$ angle of ~79°. The average Xe-F axial interatomic distance of the two crystallographically distinct species is 1.813Å and the axial Xe-F distance for each species does not depart significantly from this mean. The mean of all Xe-F equatorial interatomic distances is 1.843Å. Again there is no significant departure from this mean value for the Xe-F equatorial distances in each species.

The Xe atom of each XeF_5 group makes one short contact with one Pd-F_6 group (i.e., Xe(2) - F(3), Xe(1) - F(4)) and two somewhat longer contacts to a second PdF_6 group. These Xe...F contacts link XeF_5 and

PdF_6 groups into "rings" containing two species of each kind as shown in Fig. 2a. These "rings" are linked by the further involvement of the PdF_6 groups in adjoining "rings". There is a striking resemblance of the four member "ring" in this structure to that previously observed in $XeF_5^+AsF_6^-$.[15]

It should be noted that the three F-ligands of the PdF_6 groups which make close approach to the Xe atom do so more or less symmetrically with respect to the pseudo four-fold axis of each XeF_5 group. Thus, the F_{axial}-Xe-...F (close contact) angles all lie within the range 135-146°. The manner in which the XeF_5 and PdF_6 groups are arranged in the crystal is illustrated in the stereogram, which is Fig. 2c.

D. Discussion

1. Structure Analysis[23]

The analysis was hampered by the fact that the structure deviates only a little from space group Pcan (No. 60, with an unconventional setting).[17] The coordinates of Xe and F listed in Table I can be grouped as pairs related by the transformation x, 1/2 - y, 1/2 - z with discrepancies no greater than 0.046 for F and 0.023 for Xe, while Pd would be related to itself by this operation if its y were increased by 0.008. If this correspondence were exact, the symmetry would be Pcan, a centric space group. This pseudosymmetry escaped notice at first because there are clear violations of the extinction rule for the n glide. The structure consisting of Xe(2) atoms is nearly the inverse of that of the Xe(1) atoms, and thus has the same Patterson vectors. As a result, it was easy to find vectors for two sets of four heavy atoms per unit cell in the Patterson maps, but a third set could not be found. If one tries to

interpret these vectors in space group Pcam (the centric group consistent with the extinction rules) either set of four atoms can be placed on the mirror planes, but then the other must be in a general set of positions. This interpretation was ruled out by the absence of vectors for such atoms related by the mirror. Had the similarity to space group Pcan been noticed, it would have been easy to assign four Pd atoms to a special position (on the two-fold axis) and eight Xe atoms to a general position.

The next complication is that Pd hardly contributes to the phasing of any reflection with $\underline{h} + \underline{k}$ odd, nor Xe to any reflection with $\underline{\ell} = 0$ and $\underline{h} + \underline{k}$ odd. For other reflections the heavy atoms give good phasing for the centric pseudostructure, but the deviations from this symmetry will be controlled by the accident of the slight displacements of the trial structure. Thus the heavy atom positions are not a very helpful guide to the correct positions of the F atoms, and false minima with relative good agreement indices are possible. A similar situation was encountered in the refinement of the structure of $Na_4XeO_6 \cdot 6H_2O$.[24]

A third difficulty is the question of absolute polarity. The structure is too nearly centric for there to be any dramatic differences in the Bijvoet pairs, and the differences in agreement indices are not very decisive. It is even more difficult to exclude the possibility of two orientations mixed by twinning. Had the measurements been confined to one octant, as is often the custom, the polar dispersion effect[25,26] would have caused a serious uncertainty. With full data that effect disappears, and nearly the same results are obtained with either assumption of polarity.

2. Chemical Aspects

Hexafluoropalladates(IV) have long been known[27] and a regular octahedral PdF_6^{2-} geometry was indicated by the isomorphism of the alkali fluoropalladates with the fluoroplatinates, of which the crystal structure of K_2PtF_6 was known from X-ray single crystal structure analysis.[28] Hithertoo, however, the only structure determination reported for a PdF_6^{2-} salt was that of Bartlett and Quail,[3] derived for K_2PdF_6 from X-ray powder data. Although the precision of their structure is uncertain, the quoted Pd-F bond length of 1.86Å is roughly compatible with the Pd-F bond lengths observed in the $[XeF_5]_2PdF_6$ structure (see Fig. 1 and Table III).

The structure of $[XeF_5]_2PdF_6$ is of most interest at this time for the geometry of the cation and the cation coordination. The cation has previously been established by X-ray single crystal analysis in the salts $XeF_5^+MF_6^-$ (M = Pt and Ru (Ref. 14), As (Ref. 15)) and crystalline XeF_6 itself has been formulated[29] as $XeF_5^+F^-$. Table IV gives the bond lengths and angles for the various structures examined so far. It can be seen that within the quoted standard deviations, there are barely any significant differences between XeF_5^+ species in different lattices, including XeF_5^+ in crystalline XeF_6. As has already been pointed out above, the two crystallographically distinguishable XeF_5^+ species in $[XeF_5]_2PdF_6$ are not significantly different. As may be seen from Table IV, the precision of the XeF_5^+ description from this structure is quite high. The common geometry of XeF_5, in all of the quoted structures, itself suggests a discrete cation, but as has been pointed out previously[14,30] the close similarity to the neutral molecule IF_5 provides

compelling evidence. Indeed, the strictly isoelectronic relatives of XeF_5^+ are remarkably similar in shape to it (see Table V).[18] This highlights the constancy of the bond angle angle F_{axial}-E-$F_{equatorial}$.[18]

The coordination behavior of the XeF_5^+ species not only supports the discrete nature of the species but also provides evidence of steric activity of the Xe(VI) non-bonding valence-electron pair. Figures 1 and 2 show that each XeF_5 species in $[XeF_5]_2PdF_6$ is coordinated to three F ligands of two PdF_6 groups, such that the three F ligands lie approximately on a conical surface, the axis of which is coincident with the symmetry axis of the XeF_5. But if we describe XeF_5^+ as a pseudo-octahedral species in which the non-bonding valence-electron pair occupies the Xe-coordinate site <u>trans</u> to the axial bond, the position of the F ligands "on the conical surface" is seen to be appropriate, since then the Xe-valence "pair" is avoided, and the positive charge of the cation (anticipated to be centered essentially at the xenon atom) is least shielded. This model does not, of course, allow the prediction that three F ligands would coordinate to each XeF_5^+ and indeed in $XeF_5^+PtF_6^-$ and $XeF_5^+RuF_6^-$ (Ref. 14) the cation coordinate in anion F ligands is four, not three.

It is not yet clear why certain anions (like PtF_6^- and RuF_6^-) provide four F ligands to coordinate to XeF_5^+, whereas PdF_6^{2-} and AsF_6^- (Ref. 15) provide three. The similarity of the XeF_5^+ coordination in the PdF_6^{2-} and AsF_6^- salts is striking. As a consequence, essentially the same ring (shown for $[XeF_5]_2PdF_6$ in Fig. 2) of two XeF_5 groups linked to two MF_6 groups occurs in each structure. It is of relevance to the hypothesis of steric activity of the non-bonding Xe(VI) valence electron

"pairs" that the XeF_5 groups do not share a common axis in the ring but avoid one another (see the stereogram, Fig. 2b).

It appears probable that the $2XeF_6 \cdot MF_4$ (M = Ge, Sn) complexes reported[31] by Pullen and Cady, will prove to be structurally related to $(XeF_5^+)_2PdF_6^{2-}$. The ability of XeF_6 to donate F^- to a tetrafluoride to form $(XeF_5^+)_2PdF_6^{2-}$ indicates that it is a moderately good base. It remains, however, to be seen if $(XeF_5^+)_3MF_6^{3-}$ salts can be derived from the metal trifluorides.

Table I. Positional and thermal parameters for $[XeF_5^+]_2PdF_6^{2-}$ with estimated standard deviations in parentheses.

ATOM	X	Y	Z	B11	B22	B33	B12	B13	B23
PD	.17525(7)	.24185(6)	.250*	2.70(3)	2.53(3)	1.13(2)	-.25(3)	-.02(3)	.22(3)
XE(1)	.53535(7)	.12057(5)	.0332(1)	3.11(3)	3.24(3)	1.75(3)	.75(2)	-.10(2)	.29(3)
XE(2)	.51278(7)	.38670(6)	.4738(1)	2.85(3)	3.20(3)	1.82(3)	-.58(3)	-.20(2)	.49(3)
F(1)	.0394(6)	.2865(5)	.3880(8)	4.0(3)	3.1(3)	1.3(3)	.9(2)	.5(2)	-.2(3)
F(2)	.0268(6)	.2145(5)	.1235(8)	3.8(3)	2.5(3)	1.5(3)	-.1(2)	-.5(2)	-.0(2)
F(3)	.3261(7)	.2720(6)	.3796(8)	3.8(3)	5.4(4)	1.7(3)	-1.7(3)	-.9(2)	1.1(3)
F(4)	.3101(6)	.1917(6)	.1150(8)	3.5(3)	6.8(4)	1.8(3)	1.7(3)	.9(2)	1.0(3)
F(5)	.1555(7)	.1085(5)	.3352(7)	4.1(3)	2.4(3)	2.0(3)	.1(2)	.4(2)	.7(2)
F(6)	.1809(7)	.3767(5)	.1659(8)	4.6(3)	2.6(3)	2.4(3)	-.8(2)	-.2(2)	.9(2)
F(7)	.4920(9)	-.0171(5)	-.001(1)	8.7(4)	2.2(3)	4.9(5)	.6(3)	-1.6(3)	.8(3)
F(8)	.7048(8)	.0634(7)	.0830(9)	4.7(4)	8.6(5)	5.0(5)	3.6(4)	-1.1(3)	.3(4)
F(9)	.6348(8)	.1241(6)	-.1368(8)	4.2(3)	5.8(4)	2.9(3)	1.7(3)	1.7(3)	.4(3)
F(10)	.6289(9)	.2376(6)	.0990(8)	5.5(4)	6.5(4)	2.7(4)	-1.5(3)	-1.7(3)	-.5(3)
F(11)	.5049(9)	.0869(8)	.2209(9)	7.3(5)	8.9(5)	1.9(4)	3.5(4)	.7(3)	2.6(4)
F(12)	.6658(8)	.4658(6)	.4212(9)	4.9(4)	6.8(5)	4.9(5)	-2.6(3)	-.1(3)	1.7(4)
F(13)	.4460(8)	.5180(5)	.519(1)	6.5(4)	2.9(3)	5.3(5)	-.1(3)	.2(4)	.9(3)
F(14)	.6301(8)	.2836(7)	.4013(9)	5.0(4)	6.0(4)	3.8(4)	-.2(4)	1.6(3)	-.9(3)
F(15)	.4669(9)	.4216(7)	.288(1)	8.2(5)	7.1(5)	2.6(4)	-4.0(4)	-1.7(3)	2.6(4)
F(16)	.6188(8)	.3897(6)	.6381(8)	4.2(3)	4.4(3)	2.4(3)	-.7(3)	-1.4(2)	-.1(3)

* Fixed Parameter.

Table II. Observed structure factors, standard deviations and differences (x 1.0) for $[XeF_5^+]_2PdF_6^{2-}$.

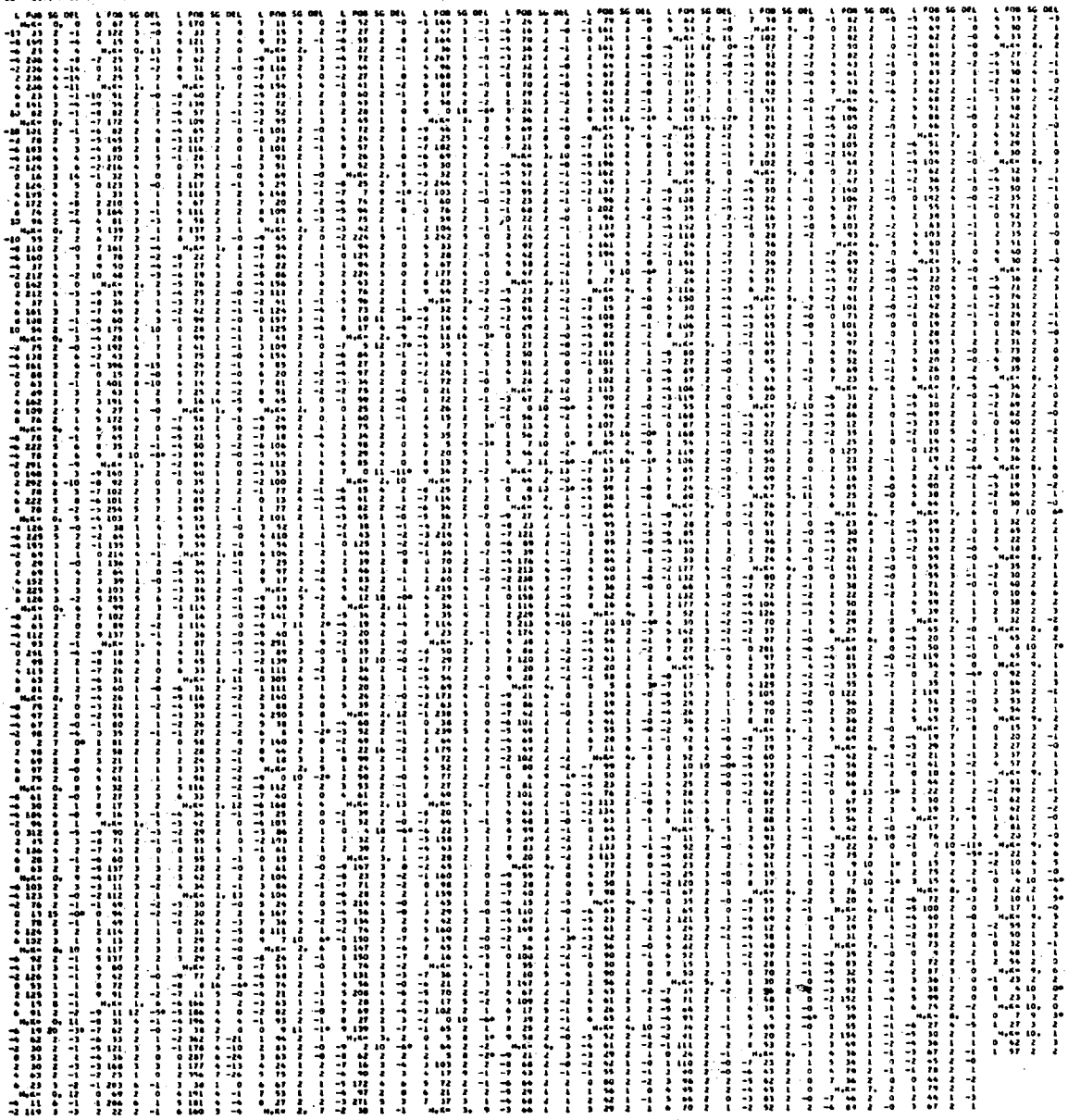

TABLE III

Interatomic Distances (Å) and Angles (Deg.) Within the $[XeF_5^+]_2PdF_6^{2-}$ Asymmetric Structural Unit

Distances		Angles			
Xe(1)-F(8)	1.806(7)	F(8)-Xe(1)-F(1)	134.21(42)	F(12)-Xe(2)-F(2)	135.92(39)
F(7)	1.836(7)	F(4)	146.39(44)	F(3)	142.70(45)
F(9)	1.849(7)	F(5)	140.21(40)	F(6)	140.82(42)
F(10)	1.841(7)	F(7)	81.45(40)	F(13)	79.79(39)
F(11)	1.838(8)	F(9)	78.06(35)	F(14)	80.20(42)
F(4)	2.418(6)	F(10)	79.93(40)	F(15)	77.98(39)
F(5)	2.582(6)	F(11)	78.02(38)	F(16)	78.02(37)
F(1)	2.617(7)				
		F(7)-Xe(1)-F(9)	88.93(52)	F(13)-Xe(2)-F(15)	85.40(46)
Xe(2)-F(12)	1.820(7)	F(11)	84.93(48)	F(16)	88.25(49)
F(13)	1.842(7)				
F(14)	1.845(8)	F(10)-Xe(1)-F(9)	91.82(41)	F(14)-Xe(2)-F(15)	87.80(49)
F(15)	1.855(8)	F(11)	86.63(48)	F(16)	90.28(41)
F(16)	1.835(7)				
F(3)	2.445(7)	F(1)-Pd-F(2)	89.66(33)	F(3)-Pd-F(4)	90.23(36)
F(6)	2.559(7)	F(3)	89.85(37)	F(5)	89.10(35)
F(2)	2.639(7)	F(5)	85.25(34)	F(6)	93.53(35)
		F(6)	91.70(34)		
Pd-F(1)	1.902(6)			F(4)-Pd-F(5)	92.45(37)
F(2)	1.860(6)	F(2)-Pd-F(4)	90.28(36)	F(6)	90.59(36)
F(3)	1.902(7)	F(5)	91.59(32)		
F(4)	1.900(7)	F(6)	85.75(35)		
F(5)	1.893(6)				
F(6)	1.898(6)				

TABLE IV

The XeF_5^+ Ion

	$Xe-F_{ax}$ ‡	Average ‡ XeF_{eq}	Average ‡ $F_{ax}-Xe-F_{eq}$	
XeF_6	(t)* 1.84(4) Å	1.86(3)	77.2(18)°	(a)
	(h) 1.76(3)	1.92(2)	80.0(6)	
$XeF_5^+AsF_6^-$	1.76(2)	1.82(3)	80.4(15)	(b)
$XeF_5^+RuF_6^-$	1.79(1)	1.85(1)	79.0(6)	(c)
$XeF_5^+PtF_6^-$	1.81(8)	1.88(8)	79.5(40)	(d)
$[XeF_5^+]_2PdF_6^{2-}$	1.81(1)	1.84(1)	79.2(4)	present work

* (t) indicates tetramer and (h) hexamer. ‡ number in parentheses are the estimated standard deviations for the least signficant digit.

(a) Reference 29; (b) Reference 15; (c) Reference 14(b); (d) Reference 14a

TABLE V

Distances (Å) and F_{ax}-E-F_{eq} Angle (Deg.) for the Isoelectronic Species EF_5 (E = Sb, Te, I, Xe), Averaged to C_{4v} symmetry for Comparison

	SbF_5^{2-} [a]	TeF_5^- [b]	IF_5 [c]	XeF_5^+
M-F_{ax}	1.916(4)	1.862(4)	1.817(10)	1.813(7)
M-F_{eq}	2.075(3)	1.952(4)	1.873(5)	1.843(8)
F_{ax}-E-F_{eq}	79.4(1)	78.8(2)	80.9(2)	79.2(4)

a R. R. Ryan and D. T. Cromer, Inorg. Chem. 11, 2322 (1972).

b S. H. Mastin, R. R. Ryan and L. B. Asprey, ibid. 9, 2100 (1970).

c G. R. Jones, R. D. Burbank and N. Bartlett, ibid. 9, 2264 (1970).

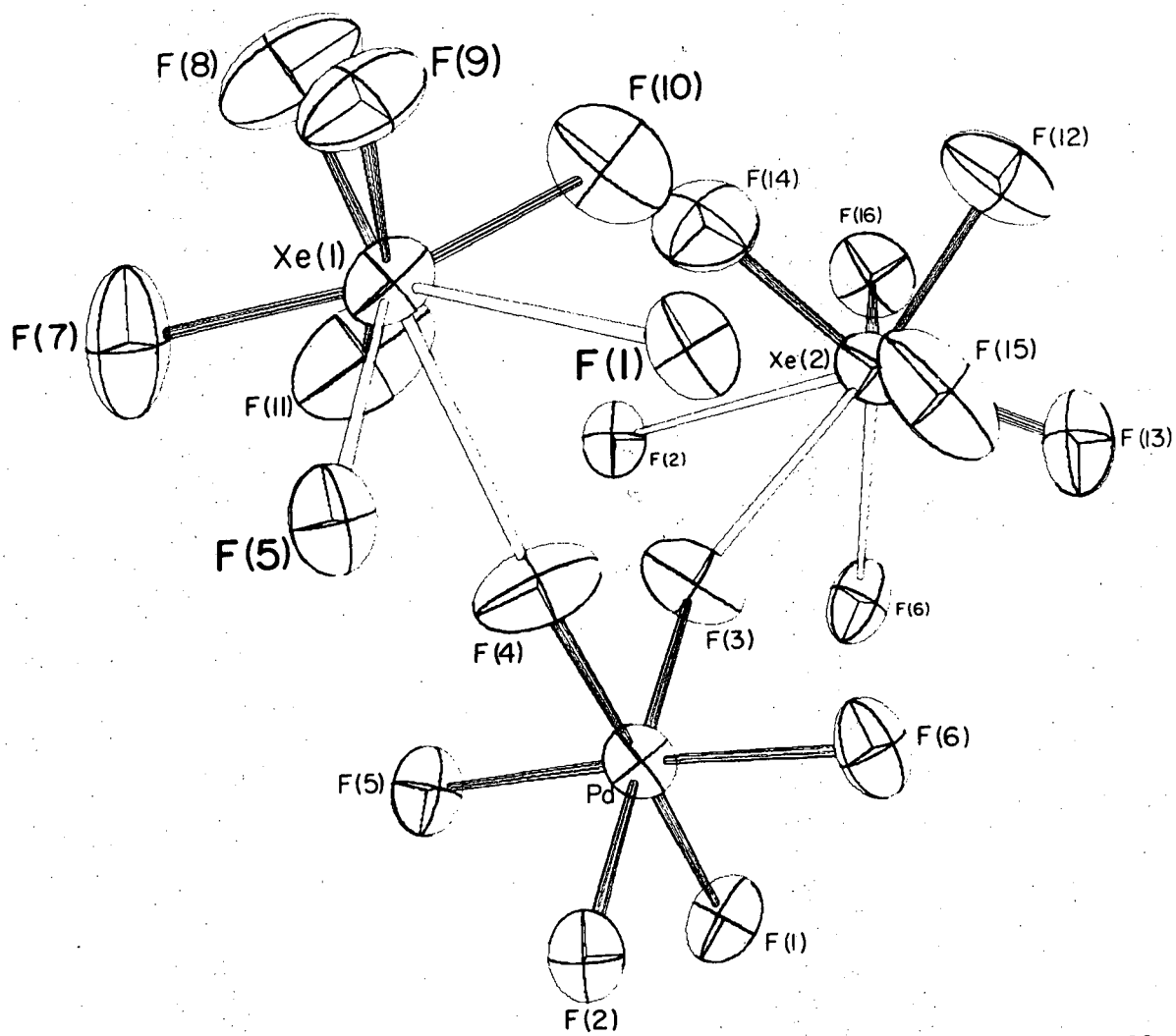

Fig. 1(a): The formula unit in $[XeF_5^+]_2PdF_6^{2-}$.

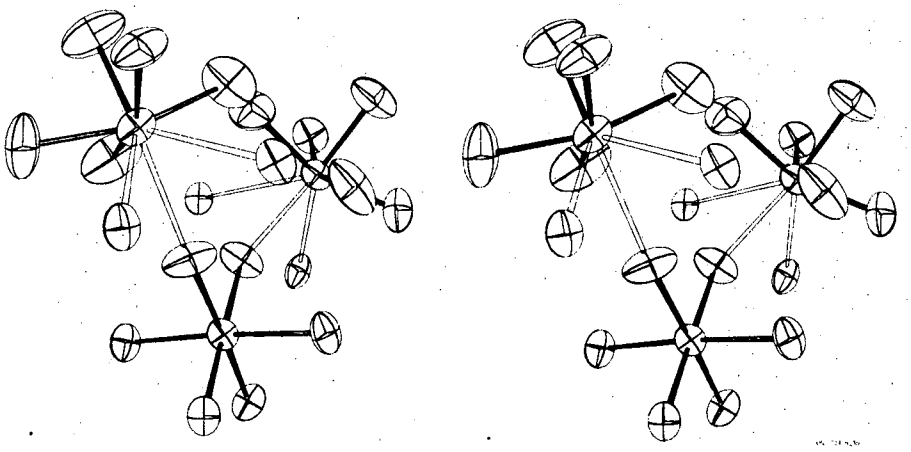

Fig. 1(b): Stereogram of the formula unit in $[XeF_5^+]_2PdF_6^{2-}$.

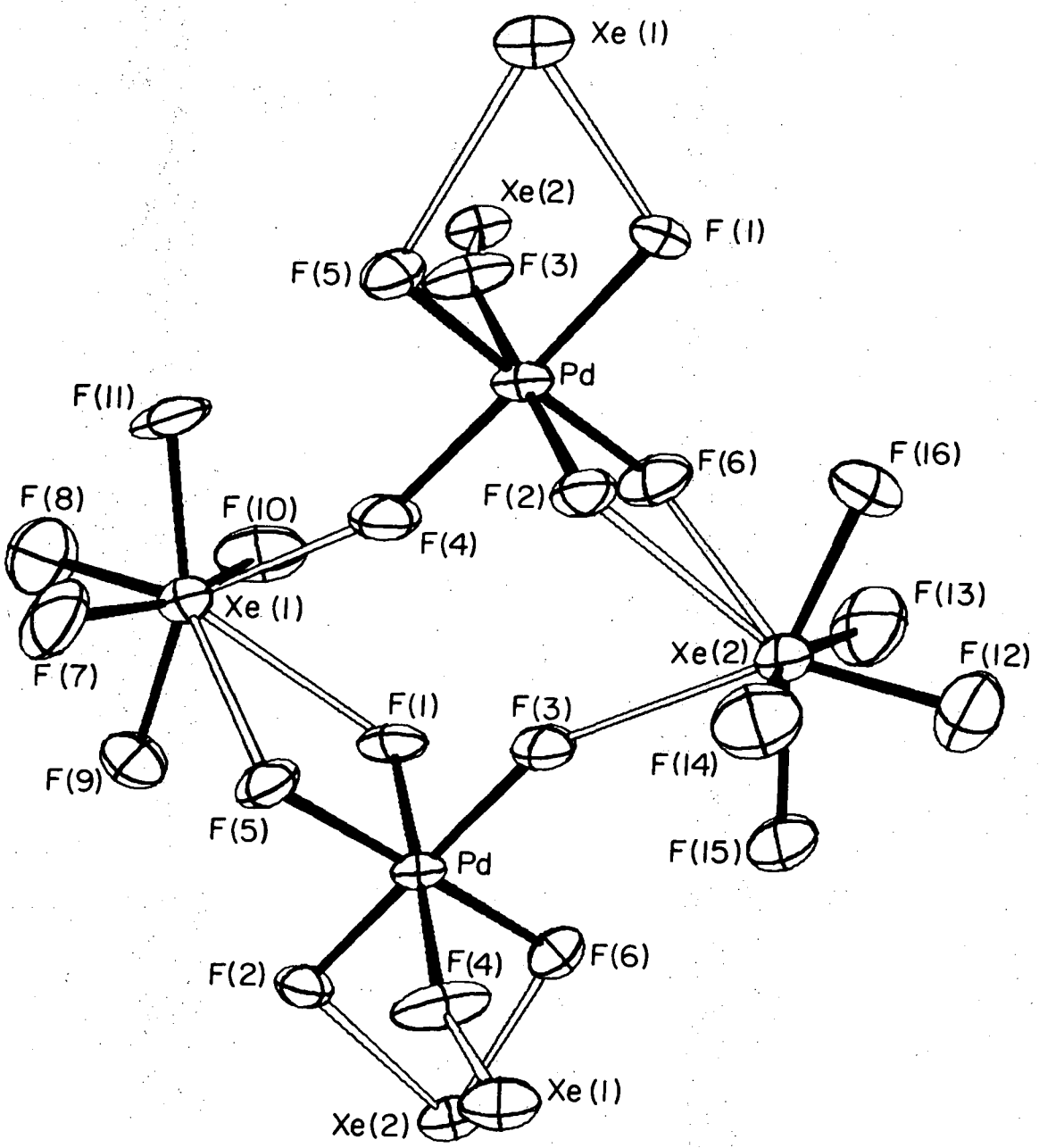

XBL 725-6264

Fig. 2(a). The $XeF_5^+AsF_6^-$-like rings in $[XeF_5^+]_2PdF_6^{2-}$.

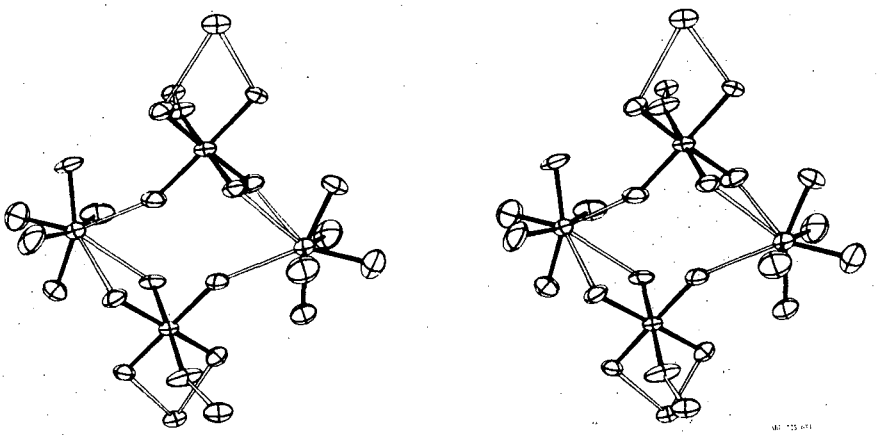

Fig. 2(b). Stereogram of the $XeF_5^+AsF_6^-$-like rings in $[XeF_5^+]_2PdF_6^{2-}$.

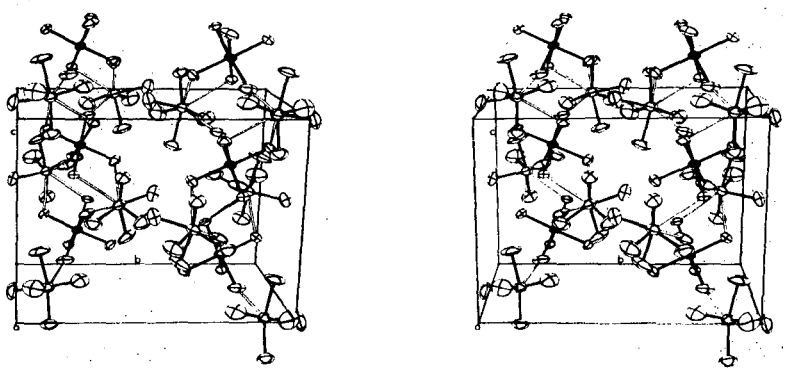

Fig. 2(c). Stereogram of the $[XeF_5^+]_2PdF_6^{2-}$ unit cell, showing the packing of linked $XeF_5^+AsF_6^-$-like rings.

IV. THE PREPARATION AND SOME PROPERTIES OF GOLD(V) COMPOUNDS

A. Introduction

The extraordinary oxidizing power of the transition metal hexafluorides has been well established for several years.[32] Indeed, Bartlett and co-workers[33] have shown that the electron affinity of the third row hexafluorides increases approximately 1 electron volt per unit increase in atomic number, from left to the right across the period, and recent thermochemical measurements by Barberi and Bartlett[34] have provided a value of -215 kcal/mole for the electron affinity of PtF_6. Thus, AuF_6, if it can be made, should have on electron affinity of ~-240 kcal/mole, and may be capable of oxidizing krypton gas spontaneously at room temperature. In addition, the AuF_6^- ion, because of its small size and high ionization potential, may stabilize ArF^+ salts.

The pattern of the known oxidation states of the second and third row transition metals, prior to the present work (shown in Table I), indicated an anomaly at gold: Pt(VI) and Pd(IV) compounds were known, but no oxidation states higher than Au(III) were characterized. These observations, coupled with some preliminary evidence obtained by Rao and Bartlett[35] for a higher fluoride of gold, indicated that it might be possible to prepare a new oxidation state of gold, the Au(V) and (VI) states being the most likely to exist.

It is common knowledge that the highest oxidation state of an element often occurs in a complex anion. One expects the electronegativity of a metal atom in a given formal oxidation state to be lower in an anion that is a neutral compound. Thus, as a first step, synthetic

efforts were directed at exploiting the known fluoride ion donor, oxidizing and solvent properties of XeF_6 in anticipation that these properties would generate the AuF_6^- ion. This rationale is similar to that employed in the attempted synthesis of Pd(V) compounds as described in Chapter II. In the gold case, however, the approach was successful, and this chapter describes the synthesis and characterization of some Au(V) compounds.

B. Experimental

Gold powder (200 mesh) was used as supplied by ROC/RIC Sun Valley, CA 99.9% pure. Oxygen gas of reagent grade from the Pacific Oxygen Company, Oakland, CA was purified by passing it through traps at -183°C. Fluorine gas, bromine trifluoride, bromine pentafluoride and iodine pentafluoride were obtained from the Matheson Company, East Rutherford, NJ. Volatile impurities were removed from the fluorine at pressures up to 2 atmospheres by trapping at -183°. BrF_3, BrF_5 and IF_5 were purified by treatment with fluorine gas at room temperature followed by trap to trap distillation. Gas phase infrared spectroscopy was used to monitor their purity. Nitric oxide was supplied by the Matheson Company and was purified by fractional distillation. Its purity was checked using infrared spectroscopy. Cesium fluoride (Alfa Inorganic, Beverly, MA) and potassium fluoride (Allied Chemical, Morristown, NJ) were dried at 200°C and stored in the Dri-Lab. X-ray powder photographs were used to check for bifluoride and other impurities. Antimony pentafluoride of Spectrograde quality was used as supplied by Cationics, Inc., Cleveland, OH. Xenon difluoride was prepared using the method described in Chapter II. Nitrosyl Chloride[36] and IF_5SBF_5[37,38] were prepared as previously described.

BrF_3AuF_3 and AuF_3 were prepared using Sharpe's method.[39] The trifluoride was subsequently treated with F_2 at 60 psi and 320° to remove any trace of bromide. $Cs^+AuF_4^-$ and $K^+AuF_4^-$ were prepared by dissolving equimolar amounts of CsF or KF and AuF_3 in BrF_3 solvent in a quartz reactor. $NO^+AuF_4^-$ was prepared using a slight modification of Woolf's method,[40] in which AuF_3 was used as a starting material instead of Au powder.

1. Preparation of $Xe_2F_{11}^+AuF_6^-$

Typically, 1.5 g AuF_3 (5.9 mmoles) and 3.0 g XeF_2 (17.8 mmoles) were placed in a monel bomb. Fluorine gas (70 mmoles) was condensed into the bomb which was then heated to 400°C for 36 hr. After slowly cooling to room temperature, excess F_2 and XeF_6 were removed under vacuum, and the bomb was opened in the Drilab, yielding a macrocrystalline mass of yellow-green material. This solid melted without decomposition at 145-150°C. It reacted explosively with water.

In order to place a reasonable lower limit on the synthetic conditions, $Xe_2F_{11}^+AuF_6^-$ was also prepared by heating 1.5 g AuF_3 (5.9 mmoles) 3.0 g XeF_2 (17.7 mmole) and F_2 (45.4 mmoles) (which is the stoichiometricly required amount plus a 10% excess) to 260° for 24 hr in a 50 ml monel bomb. The product, which was poorly crystalline, was identified as $Xe_2F_{11}^+AuF_6^-$ by Raman spectroscopy and an X-ray powder photograph.

Analysis for Xe was by the modified Dumas method: Found: Xe, 33.2±0.4%. Required for $Xe_2F_{11}^+AuF_6^-$, Xe 33.5%.

X-ray powder photographs indicated $Xe_2F_{11}^+AuF_6^-$ to be isomorphous with $Xe_2F_{11}^+MF_6^-$, M = Ru, Ir, Pt.[5,42]

A full single crystal X-ray structural analysis in space group Pnma has been completed,[43] and is reported in Chapter V.

The Raman spectrum of $Xe_2F_{11}^+AuF_6^-$ is shown in Fig. 1.

2. Preparation of $XeF_5^+AuF_6^-$

$XeF_5^+AuF_6^-$ was prepared from $Xe_2F_{11}^+AuF_6^-$ by heating the 2:1 compound to 110°C under vacuum in a Kel-F trap. The 1:1 compound was purified by sublimation at this temperature, yielding a pale yellow-green solid which melted without decomposition to a clear greenish-yellow liquid at 190-192°C. This compound also reacted explosively with water.

Analysis for Xe gave the following: Found: Xe, 25.2±0.5%; required for $XeF_5^+AuF_6^-$, Xe 24.4%

X-ray powder photographs showed that the 1:1 compound was not isomorphous with $XeF_5^+MF_6^-$ salts where M = Os, Ir, Pt, Ru but that it was isomorphous and nearly isodimensional with $XeF_5^+AsF_6^-$.[15] Single crystal data[44] showed $XeF_5^+AuF_6^-$ to be monoclinic with a = 5.88(2)Å, b = 16.54(2) c = 8.35(2), β = 90.1(1)°, V = 812.1Å^3, z = 4, D_{calc} = 3.40 g/cm^3. Systematic absences indicated the space group $P_{2_{1/c}}$.

No evidence was found for a 1:2 product (i.e., $XeF_5^+Au_2F_{11}^-$).

3. Preparation of $CsAuF_6$[41]

Typically, 0.80 g $Xe_2F_{11}^+AuF_6^-$ (1.02 mmoles) and 0.17 g CsF (1.12 mmoles) were mixed intimately, then transferred to a small Monel crucible contained in a quartz tube. The mixture was heated to 110° under 1 atm dry nitrogen at which temperature reaction occurred. The evolved XeF_6 was removed under vacuum, leaving a pale yellow solid which reacted rapidly with water, liberating ozone smelling gases and forming gold(III) hydroxide. $CsAuF_6$, $KAuF_6$ and $NO^+AuF_6^-$ can also be prepared by direct fluorination of the respective AuF_4^- salt in a Monel bomb at 350° and 1000 psi F_2. All of

these compounds were pale yellow solids. All are rhombohedral with: for $CsAuF_6$, a = 5.24(1)Å, α = 96.43(5)°; $KAuF_6$, a = 4.946(5)Å, α = 97.96(3)°; $NOAuF_6$, a = 5.05(1)Å, α = 98.82(5)°. The X-ray data showed that all three compounds were isomorphous with their analogous noble metal salts.[45] The powder data is tabulated in Tables II through IV. The infrared spectrum of solid $CsAuF_6$ showed one band at 640 cm^{-1} (assigned to ν_3 of AuF_6^-) Raman spectra of these compounds are shown in Fig. 1. The data are tabulated in Table VI. $NO^+AuF_6^-$ decomposed at 400°C to yield $NO^+AuF_4^-$ and F_2. The reaction was performed in a Monel can, and the evolved F_2 was detected using KI. An IR spectrum of the gases produced showed no ONF or ONF_3. The $NO^+AuF_4^-$ was identified by its Raman spectrum and powder photograph.

4. Reaction of $NO^+AuF_6^-$ with NO

NO reduced $NO^+AuF_6^-$ dissolved in IF_5 to Au metal at 0°C. The other product was $NO^+IF_6^-$. No evidence for a product of intermediate composition (e.g., $(NO^+)_2AuF_6^=$) was indicated.

5. Preparation of $O_2^+AuF_6^-$ [41]

Typically, 0.50 g AuF_3 (1.97 mmoles) was placed in a nickel liner in a prefluorinated Monel bomb, oxygen (18 mmoles) and fluorine (49 mmoles) were then condensed into the bomb which was subsequently heated to 500°C for 48 hr, then cooled slowly to room temperature. The product (which reacted vigorously with water) was a pale yellow-green solid. The magnetic susceptibility of $O_2^+AuF_6^-$ (5°K → 98.5°K) was obtained on a Princeton Applied Research vibrating sample magnetometer. The material exhibited Curie-Weiss behavior, with C = 0.340 cm^3 deg/mole, Θ = -3.0°K and μ_{eff} = 1.66 BM.

X-ray powder photographs showed that $O_2^+AuF_6^-$ was rhombohedral $a = 5.00(1)\text{Å}$, $\alpha = 99.95(5)°$, and that it is isomorphous with the rhombohedral form of O_2PtF_6.[46] The data is given in Table V. The Raman vibrational data is shown in Fig. 2 and Table VI.

6. Reaction of $O_2^+AuF_6^-$ and IF_5

$O_2^+AuF_6^-$ reacted with IF_5 at room temperature producing O_2, $IF_6^+AuF_6^-$ and AuF_3. The solid products were identified using Raman spectroscopy and X-ray powder photography. This reaction was similar to those previously observed between $O_2^+MF_6^-$ salts and IF_5.[47] $IF_6^+AuF_6^-$ is a yellow solid, the X-ray powder photograph of which indicated it to be cubic, with $a_o = 9.573\text{Å}$, $V = 877\text{Å}^3$, S.G. Pa_3, $z = 4$ and isostructural with $IF_6^+AsF_6^-$ ($a_o = 9.4935$, $V = 855.6$). Raman spectra and powder data for $IF_6^+AuF_6^-$ are given in Tables VI and VII .

7. Reaction of $KAuF_6$ with $IF_5 \cdot SbF_5$

$KAuF_6$ and $IF_5 \cdot SbF_5$, mixed in 1:2 molar ratio and dissolved in IF_5 at room temperature yielded IF_6^+ salts and AuF_3 (in addition to KSb_nF_{5n+1} species). The products were identified using Raman spectroscopy.

8. Attempts to Isolate AuF_5

High pressure fluorination of AuF_3. Attempts were made to fluorinate AuF_3 at pressures of 1000-1500 psi F_2 and at temperatures from 200-600°C. In the preparation at 600°C, small amounts of $O_2^+AuF_6^-$ were found, presumably due to small amounts of oxygen in the fluorine supply. No ponderable quantity of a higher binary fluoride of gold was detected.

9. Attempted Displacement of AuF_5 from AuF_6^- Salts with SbF_5

$Xe_2F_{11}^+AuF_6^-$ and $K^+AuF_6^-$ were reacted with liquid SbF_5 in an attempt to displace AuF_5 and form SbF_6^- salts.

In the experiments with $Xe_2F_{11}^+AuF_6^-$, the salt dissolved in the SbF_5, on gentle heating, to give a red solution. No fluorine was liberated from these solutions at temperatures up to 60°C. Removal of the SbF_5 under vacuum yielded on orange solid residue of soapy texture and a pale orange distillate. The solid residue gave powder patterns very similar to that of $XeF_5^+Sb_2F_{11}^-$, and Raman spectra indicated that the product may contain an $[F_5Au\text{-}F\text{-}SbF_5]^-$ mixed anion species. Raman spectra of the pole orange distillate showed only the presence of SbF_5. The presence of some gold containing species in the distillate was indicated by the pale orange color, and the gold mirror produced when the glass ampoule was sealed off under vacuum. Vigorous heating during removal of the SbF_5 gave as solid products AuF_3 and $XeF_5^+Sb_2F_{11}^-$. The same orange colored distillate was produced as described above.

It was found that $KAuF_6$ was virtually insoluble in SbF_5, even with gentle heating; consequently, a mixture of $KAuF_6$ in liquid SbF_5 was heated to 100°C under 1-2 atm of inert gas before any reaction occurred, as demonstrated by the formation of a reddish solution. Fluorine was liberated at this temperature, however. The system was heated to 200°C, but not all the $KAuF_6$ dissolved, even under these vigorous conditions. The bulk of the SbF_5 was removed under vacuum at 50°C. The last traces were removed under vacuum at 100°C. Again, two products were obtained: a pale orange distillate similar in behavior and appearance to that described above and a solid which appeared to contain an orange phase and a colorless phase. Raman spectra of the orange distillate showed only SbF_5. The solid residue had a two phase powder pattern: one phase closely resembled $O_2^+Sb_2F_{11}^-$; the other phase was unidentified.

No AuF_3 was observed. The Raman spectrum of the solid residue contained bands attributable to Sb-F stretches and Au-F stretches. Again, vigorous heating during removal of the SbF_5 gave AuF_3 and KSb_2F_{11}. A pale orange distillate similar to that described above was also obtained.

A mixture of AuF_3 and liquid SbF_5 was vigorously heated with a heat gun in an attempt to effect solution of the trifluoride, which is only sparingly soluble in SbF_5. An orange solution was obtained. A Raman spectrum of this solution showed only SbF_5. The SbF_5 was removed from this solution under vacuum, yielding two products; an orange solid, identified from its powder pattern as AuF_3, and a pale orange distillate that gave a gold mirror when the glass ampoule containing it was sealed off. A Raman spectrum of this distillate showed only SbF_5.

C. Results and Discussion

Our experiments have demonstrated that AuF_6^- salts are relatively easy to prepare. The oxidizing conditions are certainly more strenuous than for the other quinquevalent hexafluoroanions in the third transition series; indeed, progressively more potent oxidizing conditions are required with increase in the atomic number of the metal atom.[33,49]

The oxidation of gold(III) to gold(V) is an example of the classic square-planar d^8 to octahedral d^6 oxidative addition. Presumably, the AuF_6^- ion has a low spin dt_{2g}^6 configuration similar to that found in $PdF_6^=$ and $PtF_6^=$ salts with which it is isoelectronic.

The octahedral symmetry of the anion is indicated by the rhombohedral symmetry of the alkali hexafluoroaurates which are evidently isostructural with $KOsF_6$.[50] The anion in $Xe_2F_{11}^+AuF_6^-$ is nearly octahedral[43] (Chapter V) and the Mossbauer spectra[51] (Chapter VI) all slow a single narrow resonance consistent with octahedral AuF_6^-.

Both AuF_4^- and AuF_6^- salts are pale yellow to yellow-green in color; the Au-F distance in $K^+AuF_4^-$, 1.95(2)Å[52] is appreciably longer than in $Xe_2F_{11}^+AuF_6^-$, 1.86(1)Å,[43] which is in accord with the lower oxidation state of the former. The vibrational spectra are very similar: the totally symmetric "breathing" mode stretching frequencies are separated by only 7 cm^{-1}. Comparable behavior has been observed in the spectra of $[Pd(Pt)X_4]^{2-}$ and $[Pd(Pt)X_6]^{2-}$ salts,[53] and Wharf and Shriver[54] have reported similar results for SnX_3^-, SnX_4 and $SnX_6^=$ compounds.

The vibrational data for Au(V) salts, given in Table VI, confirm that the AuF_6^- ion is octahedral--ν_1, ν_2 and ν_5 were observed in the Raman, and ν_3 was observed in the infrared (due to window cutoff, ν_4 was not seen in the IR). However, in a high resolution vibrational study of XeF_5^+ salts,[35] ν_3 and ν_4 of AuF_6^- were observed in the Raman because of the small, non-centric deviation from octahedral symmetry in that compound. The results of that study are given in Table VIII. The value obtained for the totally symmetric stretching frequency (ν_1) follows the trend set by the other third row hexafluoroanions:[56] OsF_6^-, 690 cm^{-1}; IrF_6^-, 672 cm^{-1}; PtF_6^-, 647 cm^{-1}; AuF_6^-, 595 cm^{-1}. For these species, the decrease in the frequency of ν_1 with increasing atomic number has been explained by Bartlett[57] to be the result of the filling of π^* orbitals, e.g., WF_6 can be represented as having, in addition to six sigma bonds, three W-F $p\pi$-$d\pi$ bonds. The π^* orbitals in WF_6 are empty, but these orbitals are fully occupied in AuF_6^- which is accordingly a non-π bonded species.

Unit cell parameters for AuF_6^- and related MF_6^- salts are compared in Table VII. Complete tabulations of the X-ray powder data are listed in Tables II through V. The AuF_6^- ion is the smallest of the third row transition series hexafluoroanions, as shown by the unit cell volumes

for the $Cs^+MF_6^-$ series. The M-F distances in $XeF_5^+PtF_6^-$, 1.89Å,[14] and in $Xe_2F_{11}^+AuF_6^-$, 1.86Å,[43] show the anticipated decrease with increase in the atomic number of M. Evidently the increasing nuclear change effect outweighs the loss of π bond order in going from left to right across the period.

The formula unit of $O_2^+AuF_6^-$ is 4.4Å^3 smaller than that of $NO^+AuF_6^-$. The difference for the related cubic PtF_6^- salts is 3.2Å^3. Evidently, the NO^+ ion is approximately 3 or 4 Å^3 larger than O_2^+. Apparently, the effect of the greater combined nuclear changes of the atoms in O_2^+, compared with NO^+, outweighs the effect of an extra (antibonding π) electron in the former.

The small size of the AuF_6^- ion or perhaps the highly polarized nature of the F ligands in the ion may be responsible for that fact that, in a number of cases, AuF_6^- salts adopt a structure atypical of its third transition series relatives. For example, $XeF_5^+AuF_6^-$ and $IF_6^+AuF_6^-$ are isomorphous with $XeF_5^+AsF_6^-$ and $IF_6^+AsF_6$, and not with their respective platinum metal analogues. On the other hand, $Xe_2F_{11}^+AuF_6^-$ is isomorphous with the PtF_6^- salt, which is not of the same structure type as $Xe_2F_{11}^+AsF_6^-$.[58] As shown in Table VII, the volume of AuF_6^- in $CsAuF_6$ lies between AsF_6^- and PtF_6^-.

The chemistry of the AuF_6^- ion appears to be that of a two electron oxidizer. One electron reduction, which would yield a low spin d^7 configuration, would result in a gross distortion of the octahedron. There is no evidence from the present studies that the $AuF_6^=$ ion can exist.

The AuF_6^- ion does not oxidize IF_5 in neutral solutions and it therefore appears that the $d_{t2_g}^6$ configuration confers the expected kinetic stability on the anion. However, in the presence of SbF_5, which

may form a μ-fluoro bridged species such as $[F_5Sb\text{-}F\text{-}AuF_5]^-$ or even free AuF_5, there is an immediate oxidation (at room temperature) of IF_5 to yield IF_6^+ salts. This reaction illustrates the oxidative strength of Au(V) since similar spontaneous oxidation of IF_5 to IF_6^+ at ambient laboratory temperatures has previously been observed only for O_2^+ and KrF^+ salts.[59]

$O_2^+AuF_6^-$ will also oxidize IF_5 to IF_6^+ salts at room temperature according to the following stoichiometry:

$$3IF_5 + 4\ O_2^+AuF_6^- \rightarrow 4\ O_2 + 3IF_6^+AuF_6^- + AuF_3$$

In this reaction both the cation (O_2^+) and the anion (AuF_6^-) participate in the oxidation of iodine(V)-(VII). From the observed stoichiometry of the reaction

$$IF_5 + 2\ O_2^+AsF_6^- \rightarrow IF_6^+AsF_6^- + 2\ O_2 + AsF_5 \qquad \text{(Ref. 47)}$$

it is probable that the first stage of the $O_2^+AuF_6^-$ oxidation of IF_5 may be

$$IF_5 + 2\ O_2^+AuF_6^- \rightarrow IF_6^+AuF_6^- + 2\ O_2 + \text{"}AuF_5\text{"}$$

It is reasonable to suppose that the "AuF_5" produced in the initial step quickly oxidizes IF_5 to IF_7, since AuF_3 is one of the residual products.

Au(V) salts are much more powerful oxidizers than Pt(V) salts: $NO^+PtF_6^-$ will oxidize one mole of NO, forming $(NO^+)_2PtF_6^=$; under similar conditions (at room temperature in IF_5 solution) $NO^+AuF_6^-$ will oxidize five moles of NO, forming Au metal and ONF.

The experiments with AuF_6^- salts in liquid SbF_5 indicate, at least in the $Xe_2F_{11}^+AuF_6^-$ case, that some stable Au(V) species is present

in both the distillate and the solid residue, since no fluorine is liberated from this system. The Au(V) species could be distilling as an AuF_5SbF_5 μ-fluoro bridged species. Such a species could be similar to the $NbF_5 \cdot SbF_5$ cyclic compound reported by Edwards, et al.[60] The Au(V) could also be distilling as part of an $Xe_2F_{11}^+AuF_6^-$ ion pair, in a manner similar to a steam distillation.

In the experiments with $KAuF_6$ and SbF_5, the fact that fluorine is liberated from the solutions indicates that the gold species in the distillate may be an Au(III) species, since AuF_3 dissolved in SbF_5 will also yield a distillate containing some gold species. Nevertheless, Raman spectra and powder photos suggest that some Au(V) species may still be present in the solid residues.

Falconer, et al.[61] have obtained mass spectroscopic evidence for AuF_5 by vacuum sublimation of $O_2^+AuF_6^-$ against a cold finger. Their method promises to yield gram quantities of AuF_5.[62]

Table I. List of known oxidation states of the third row transition metals.

Hf	Ta	W	Re	Os	Ir	Pt	Au
			1	1			1
2		2	2	2		2	2
3	3	3	3	3	3	3	3
4	4	4	4	4	4	4	
	5	5	5	5	5	5	5*
		6	6	6	6	6	
			7	7			
				8			

*This work.

Table II.

X-Ray Powder Data for $Cs^+[AuF_6]^-$

(rhombohedral: $\underline{a}$ = 5.24(1) Å, $\underline{\alpha}$ = 96.43(5)°, $\underline{V}$ = 141.3 Å^3, probable space group $R\bar{3}$, $\underline{Z}$ = 1)

h k ℓ	$1/d^2$ Calc.	$1/d^2$ obs.	Rel. Intensity
100	.0372	.0378	w
$10\bar{1}$	.0650	.0656	vs
110	.0838	.0844	vs
$11\bar{1}$	.1022	-	
111	.1398	-	
200	.1488	.1494	s
$20\bar{1}$	.1672	-	
$2\bar{1}\bar{1}$	.1950	.1958	s
210	.2048	-	
$21\bar{1}$	.2138	.2143	vs
$20\bar{2}$	.2600	.2607	s
211	.2702	.2703	m
$21\bar{2}$	.2972	-	
$22\bar{1}$, 300	.3348	.3352	m
220	.3352		
$30\bar{1}$	.3438	.3439	m
$3\bar{1}\bar{1}$	.3622	-	
$31\bar{1}$	.3998	.3996	m
310	.4002		

h k ℓ	$1/d^2$ Calc.	$1/d^2$ Obs.	Rel. Intensity
$22\bar{2}$	.4088	.4091	mw
221	.4100		
$30\bar{2}$	.4272	-	
$31\bar{2}$	.4550	.4554	mw
$31\bar{2}$	.4738	.4743	ms
311	.4750		
$32\bar{1}$	.5302	.5297	w
$22\bar{3}$	.5572	-	
222	.5592	-	
320	.5772	-	
$30\bar{3}$	.5850	.5843	vw
$32\bar{2}$, $40\bar{1}$	.5948	-	
400	.5952	-	
$4\bar{1}\bar{1}$	.6038	-	
$31\bar{3}$	.6222	.6219	vw

Table III.

X-Ray Powder Data for $K^+[AuF_6]^-$

(rhombohedral: $\underline{a}$ = 4.946 (5) Å, α = 97.96(3)°, $\underline{V}$ = 117.8 Å^3

probable space group $R\bar{3}$, $\underline{Z}$ = 1)

	$1/d^2$		
h k ℓ	calc.	obs.	Rel. Intensity
100	.0423	.0428	s
10$\bar{1}$	.0710	.0719	vs
110	.0982	.0991	s
11$\bar{1}$	.1133	.1142	ms
111	.1677	-----	--
200	.1692	.1700	m
20$\bar{1}$	.1843	.1850	m
2$\bar{1}\bar{1}$	.2130	.2138	m
210	.2387	-----	--
21$\bar{1}$	.2402	.2407	vs
20$\bar{2}$	.2840	.2849	m
211	.3218	.3223	vw
21$\bar{2}$	.3263	.3273	m
22$\bar{1}$, 300	.3807	.3813	ms
30$\bar{1}$	.3822		
220	.3928	.3936	vw
3$\bar{1}\bar{1}$	.3973	.3976	vw
31$\bar{1}$	.4517	-----	--
22$\bar{2}$	.4532	.4536	m
310	.4638	.4635	m
30$\bar{2}$	.4683	.4687	m

h k ℓ	$1/d^2$ calc.	$1/d^2$ obs.	Rel. Intensity
221	.4895	-----	--
$3\bar{1}\bar{2}$	.4970	.4979	m
$31\bar{2}$	.5242	.5248	m
311	.5605	.5593	vw
$32\bar{1}$	.6058	.6061	mw,b
$22\bar{3}$	.6103	-----	--
320	.6315	-----	--
$30\bar{3}$	.6390	.6389	mw
$32\bar{2}$, $40\bar{1}$	.6447	.6652	w,b
$4\bar{1}\bar{1}$	.6662		
222	.6708	-----	--
400	.6768	.6784	vw,b
$31\bar{3}$	.6813		
$40\bar{2}$	.7372	.7362	w,b
321	.7418	-----	--
411	.7478	.7502	vw,b
$4\bar{1}\bar{2}$	.7523		
410	.7735	.7718	vw
$41\bar{2}$	.8067	.8063	w,b
$32\bar{3}$	.8082	-----	--
$33\bar{1}$	.8445	-----	--
$4\bar{2}\bar{2}$	.8520	.8525	vvw,b
411, 330	.8838	.8807	vvw
$33\bar{2}$	.8898	.8906	vvw
$40\bar{3}$	.8943	-----	--

h k ℓ	$1/d^2$ calc.	$1/d^2$ obs.	Rel. Intensity
$42\bar{1}$	.9155	-----	--
$4\bar{1}\bar{3}$	.9230	.9204	vvw
322	.9367	-----	--
$41\bar{3}$	.9502	.9489	vvw
420	.9548	.9576	vvw
$42\bar{2}$	.9608		
331	1.0077	1.0158	vvw
$5\bar{1}\bar{1}$	1.0197		
$50\bar{1}$	1.0318	1.0319	vvw,b

Table IV.

X-Ray Powder Data for $NO^+[AuF_6]^-$

(rhombohedral, $\underline{a}$ = 5.05(1) Å, $\underline{\alpha}$ = 98.82(5)°, $\underline{V}$ = 124.5 Å^3, probable space group $R\bar{3}$, $\underline{Z}$ = 1)

	$1/d^2$		
h k ℓ	Calc.	Obs.	Rel. Intensity
100	.0409	.0418	vs
10$\bar{1}$	.0670	.0674	vs
110	.0966	.0974	s
11$\bar{1}$	.1079	.1089	ms
200	.1636	.1644	ms
111	.1671	-----	--
20$\bar{1}$	.1749	.1760	ms
2$\bar{1}\bar{1}$	.2010	.2027	m
21$\bar{1}$	.2306	.2313	s
210	.2341	.2346	s
20$\bar{2}$	.2680	.2688	w,b
21$\bar{2}$	.3089	.3108	m,b
211	.3194	.3200	m
30$\bar{1}$	.3646	.3676	ms,b
22$\bar{1}$,300	.3681		
3$\bar{1}\bar{1}$	.3759	.3764	w
220	.3864	.3867	w
22$\bar{2}$	.4316	.4345	w,b
31$\bar{1}$	.4351		
30$\bar{2}$	.4429	.4443	w
310	.4534	.4541	m
3$\bar{1}\bar{2}$	.4690	.4708	w,b

h k ℓ	Calc.	Obs.	Rel. Intensity
221	.4865	.4872	w
$31\bar{2}$	.4986	.5000	w
311	.5535	.5533	w
$22\bar{3}$	.5769	-----	--
$32\bar{1}$	.5874	.5859	vw,b
$30\bar{3}$	.6030	.6072	vvw
320	.6205	.6202	vvw
$4\bar{1}\bar{1}$	.6326	.6356	w,b
$32\bar{2}$,$40\bar{1}$	.6361		
$31\bar{3}$	.6430	-----	--
400	.6544	.6549	vw
222	.6684	.6669	vw
$40\bar{2}$	.6996	.7009	vvw
$4\bar{1}\bar{2}$	.7109	.7113	vvw
321	.7354	.7351	w
410	.7545	.7543	w

Table V.

X-Ray Powder Data for $O_2^+[AuF_6]^-$

(rhombohedral, $\underline{a}$ = 5.00(1) Å, α = 99.95(5)°, $\underline{V}$ = 120.1 Å^3, probable space group $R\bar{3}$, $\underline{Z}$ = 1)

h k ℓ	$1/d^2$ Calc.	$1/d^2$ Obs.	Rel. Intensity
100	.0421	.0433	s
$10\bar{1}$	.0666	.0678	s
110	.1018	.1028	m
$11\bar{1}$	.1087	.1099	m
200	.1684	.1690	mw
$20\bar{1}$	.1753	.1776	mw
111	.1791		
$2\bar{1}\bar{1}$	.1998	.2013	mw
$21\bar{1}$	.2350	.2359	s
201	.2457	.2459	m
$20\bar{2}$	.2664	.2670	w
$21\bar{2}$	.3094	.3094	ms
211	.3406	.3402	w
$30\bar{1}$	.3682	.3685	w
$22\bar{1}$, 300	.3789	.3786	mw
220	.4072	.4066	vw
$22\bar{2}$	.4348	.4348	vw
$30\bar{2}$	.4417	.4436	w
$31\bar{1}$	.4455		
$3\bar{1}\bar{2}$	.4662	.4656	vw
310	.4738	.4738	vw
$31\bar{2}$	.5014	.5011	vw
212	.5197	.5186	vvw

Table VI. Raman spectra of some AuF_6^- and AuF_4^- salts.
(Frequencies in cm^{-1}, relative intensities in parentheses)

Compound	$\nu_1 AuF_6^-$	$\nu_2 AuF_6^-$	$\nu_5 AuF_6^-$	Other Features
C_sAuF_6	595 (74)	530 (vvw)	225 (26)	ν_3 (IR data) = 640
$KAuF_6$	599 (63)		238 (20)	
			222 (6)	
$NOAuF_6$	597 (70)		230 (17)	ν_{NO^+} = 2320 (vvw)
O_2AuF_6	593 (80)		228 (24)	$\nu_{O_2^+}$ = 1833 (18)
IF_6AuF_6	595 (100+)		220 (85)	$\nu_1 IF_6^+$ = 750 (49), $\nu_2 IF_6^+$ = 726 (7), $\nu_5 IF_6^+$ = 344 (31)
$Xe_2F_{11}^+AuF_6$	590 (100)		232 (25)	See Ref. 1 for cation features
XeF_5AuF_6	591 (100)		230 (27)	" "
			226 (26)	
			220 (Sh,2)	

Compound	$\nu_1 AuF_4^-$	$\nu_4 AuF_4^-$	$\nu_3 AuF_4^-$	Other Features
$CsAuF_4$	588 (98)	561 (28)	237 (13)	
			230 (14)	
$NOAuF_4$	590 (100+)	555 (54)	270 (w,sh)	ν_{NO^+} = 2305 (12)
			228 (32)	

1. C. J. Adams and N. Bartlett, submitted to Inorg. Chem.

Table VII. Unit cell parameters for some AuF_6^- and related salts.

Compound	Struct Type	a(Å)	α(°)	V(Å^3)	Reference
$CsAsF_6$	R	5.2	96	138.4	1
$CsAuF_6$	R	5.24(1)	96.43(5)	141.3	This work
$CsPtF_6$	R	5.27	96.4	143.4	2
$CsIrF_6$	R	5.27	96.2	143.6	3
$CsOsF_6$	R	5.28	96.1	144.5	3
$CsReF_6$	R	5.28	95.9	144.7	4
$CsRuF_6$	R	5.27	96.4	143.4	5
$KAuF_6$	R	4.946(5)	97.96(3)	117.8	This work
$KPtF_6$	R	4.96	97.4	119.9	6
$KRuF_6$	R	4.97	97.4	119.4	2,7
O_2AuF_6	R	5.00(1)	99.95(5)	120.1	This work
O_2PtF_6	R	4.96	97.5	119.9	8
"	C	10.032		126.3	8
$NOAuF_6$	R	5.05	98.82(5)	124.5	This work
$NORhF_6$	R	5.02(1)	97.86(5)	123.4	9
$NOPtF_6$	R	5.03	97.6	123.5	10
"	C	10.112		129.5	11

R = Rhombohedral
C = Cubic

1. B. Cox, J. Chem. Soc. 876 (1956).
2. N. Bartlett and N. K. Jha, Noble Gas Compounds, H. H. Hyman, ed (Chicago Univ. Press, 1963), p. 23.
3. M. A. Hepworth, K. H. Jack and G. J. Westland, J. Inorg. Nucl. Chem. 2, 79 (1956).
4. R. D. Peacock, J. Chem. Soc. 467 (1957).
5. J. H. Holloway, P. R. Rao and N. Bartlett, Chem. Comm. 306 (1965).
6. N. Bartlett and D. H. Lohmann, J. Chem. Soc. 619 (1964).
7. R. Hoppe, Rec. Trav. Chim. 75, 569 (1956). E. Weise and W. Klemm, Z. Anorg. u. Allgem. Chem. 279 74 (1955).
8. N. Bartlett and D. H. Lohmann, J. Chem. Soc. 5253 (1962).
9. N. Bartlett and P. R. Rao, unpublished observation.
10. N. K. Jha, Ph. D. Thesis, Univ. of British Columbia, 1965.
11. S. P. Beaton, " " " " , 1966.

Table VIII. Raman spectrum of AuF_6^- in solid $XeF_5^+AuF_6^-$.* (Frequencies in cm^{-1}, relative intensities in parentheses.)[6]

Frequency	Assignment
591 (100)	$\nu_1(a,g)$
543 (0^+)	$\nu_2(e_g)$
534 (0^+)	
650 (9)	$\nu_3(t_{1u})$
641 (28)	
628 (22)	
623 (Sh,~10)	
296 (5)	$\nu_4(t_{1u})$
283 (1)	
273 (2)	
230 (27)	$\nu_5(t_{2g})$
226 (26)	
220 (Sh,2)	

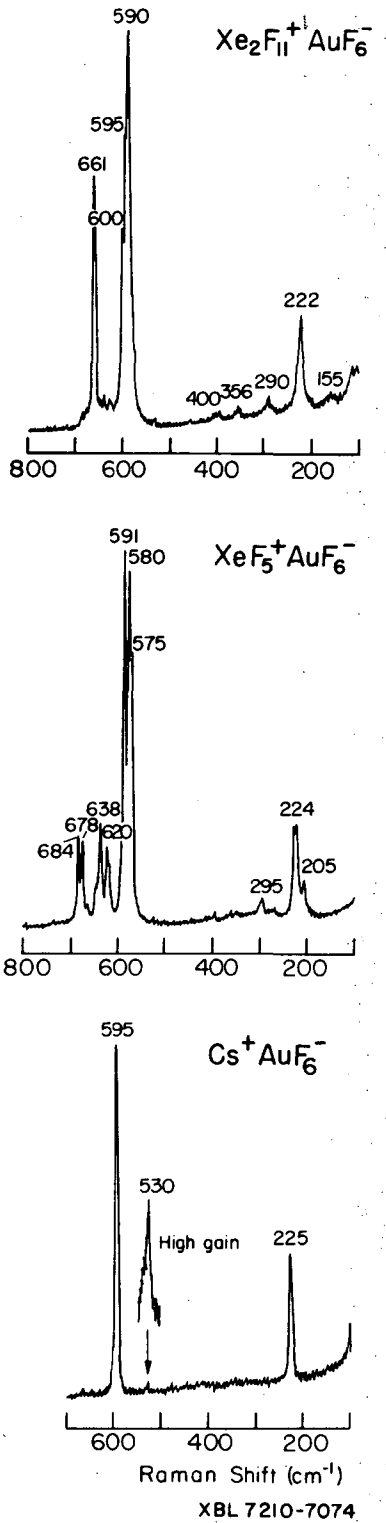

Fig. 1. Raman spectra of some AuF_6^- salts.

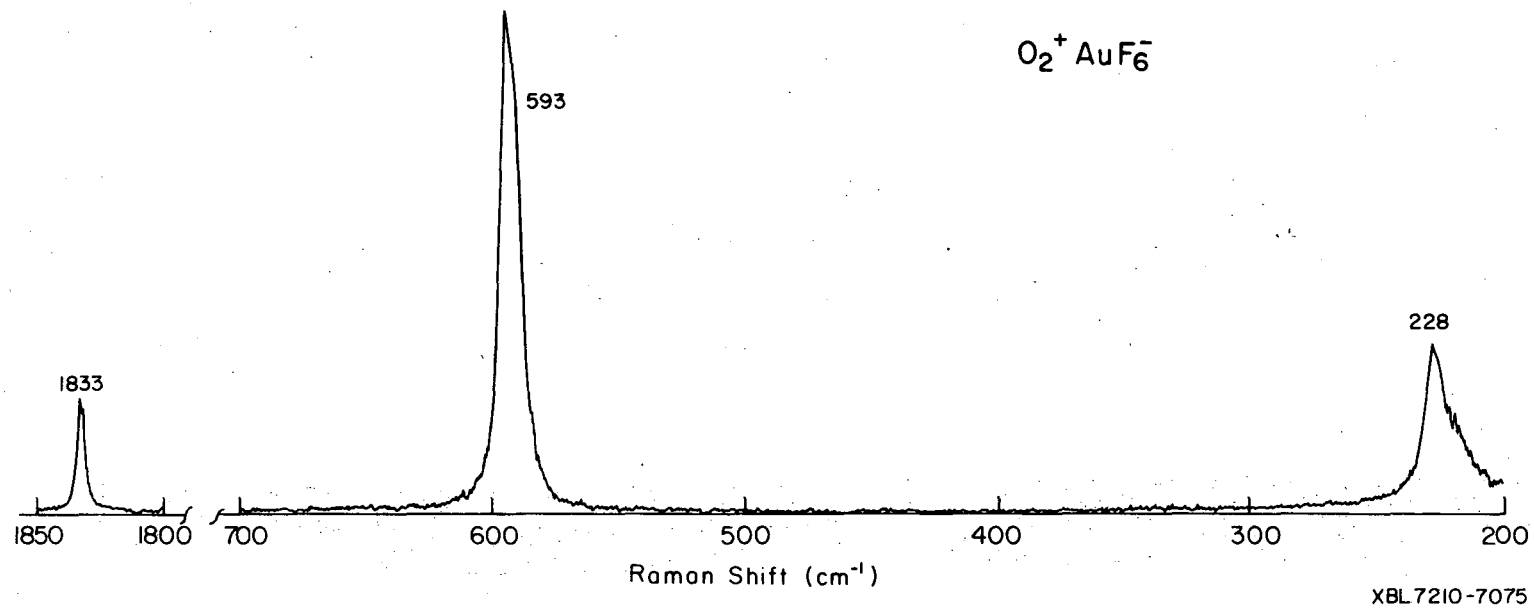

Fig. 2. Raman spectrum of $O_2^+AuF_6^-$.

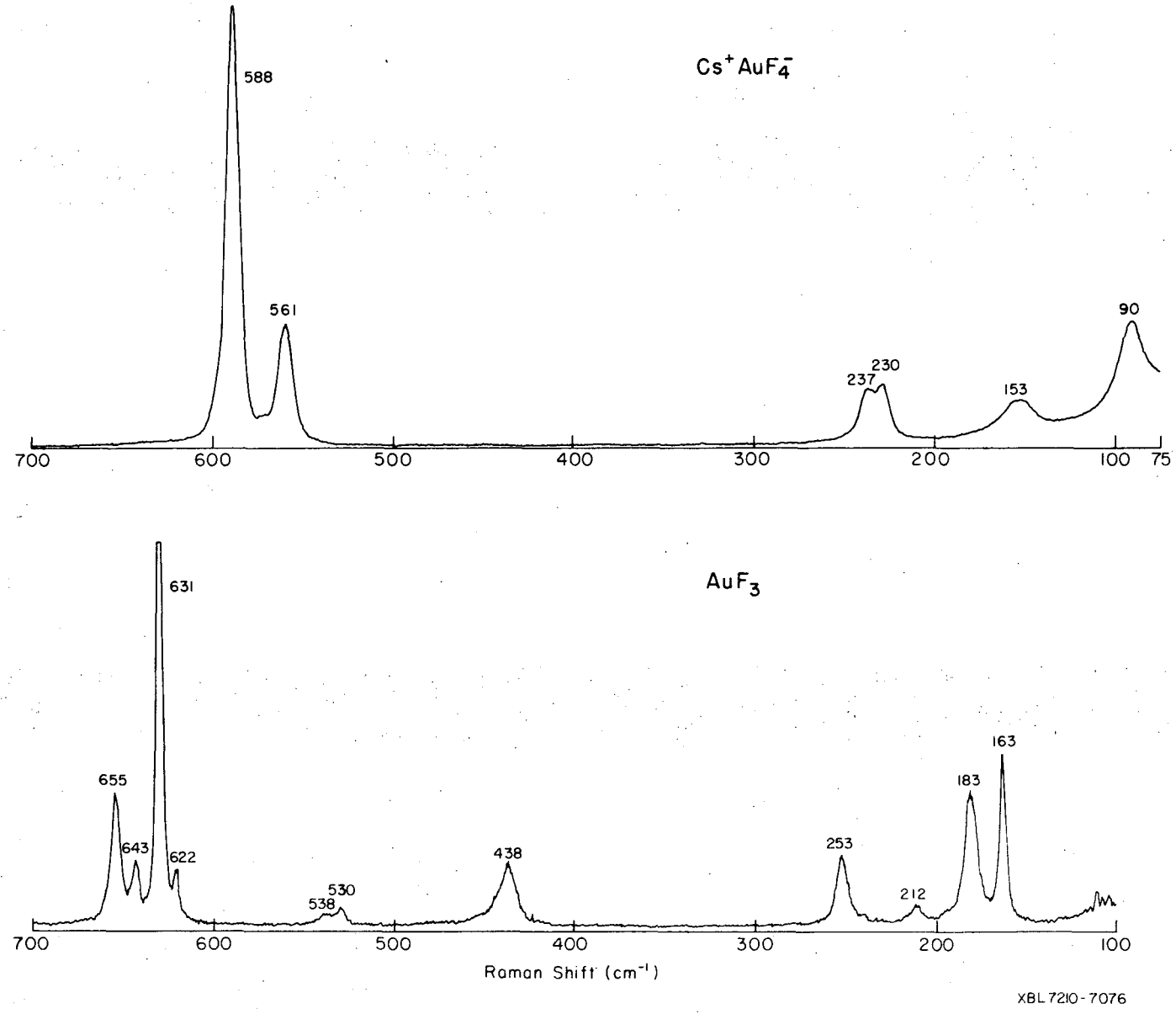

Fig. 3. Raman spectra of some Au(III) compounds.

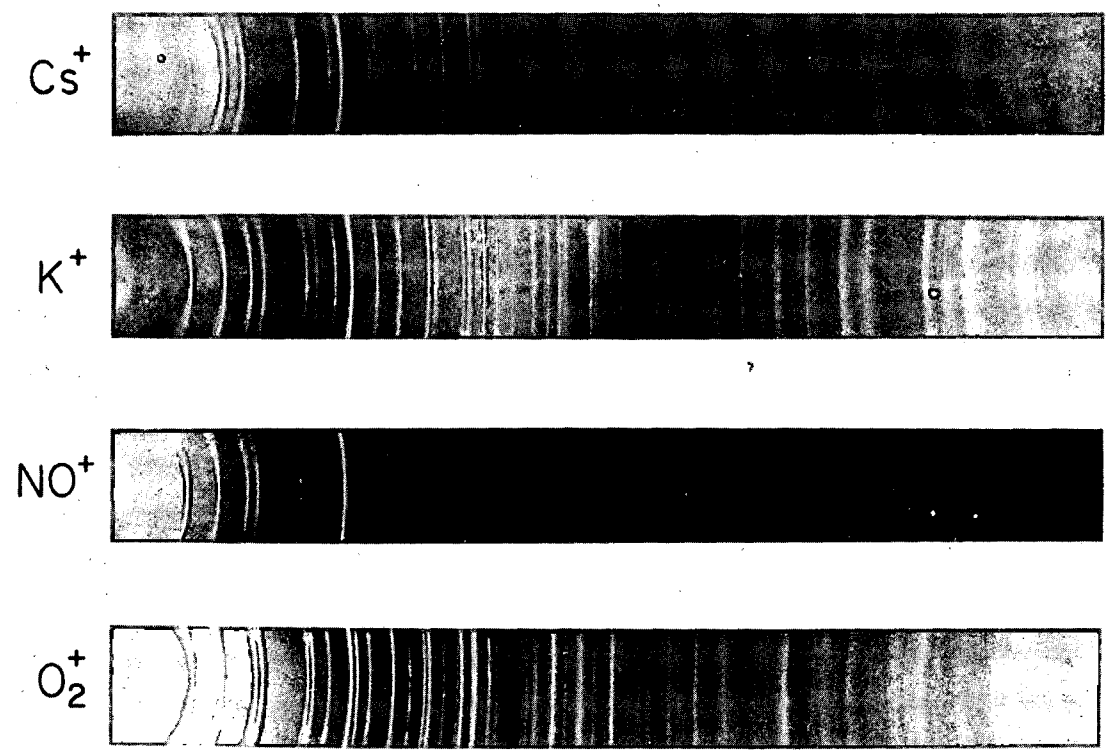

Fig. 4. XBB 754-3182

X-Ray Powder Photographs of Some AuF_6^- Salts

V. THE CRYSTAL STRUCTURE OF $Xe_2F_{11}^+AuF_6^-$ and the RAMAN SPECTRUM OF THE $Xe_2F_{11}^+$ ION

A. Introduction

$Xe_2F_{11}^+AuF_6^-$ was the first salt containing the AuF_6^- anion to be synthesized, as described in Chapter IV. Since both the cation and the anion in this compound were novel and of structural interest, fortunately the synthetic method yielded suitable single crystals for an X-ray structural analysis.

At the time they characterized the salt $XeF_5^+PtF_6^-$, Bartlett and co-workers[42,63] had also prepared a salt of empirical formula $F_{17}PtXe_2$, which they considered likely to be $Xe_2F_{11}^+PtF_6^-$. The composition of the latter, which can also be expressed as $2XeF_6 \cdot PtF_5$ adduct, suggested that the compound $2XeF_6 \cdot SbF_5$, described even earlier[64] by Gard and Cady, was also probably an $Xe_2F_{11}^+$ salt.

On the basis of Raman data[58] for $2XeF_6 \cdot AsF_5$ and $XeF_6 \cdot AsF_5$ and the crystal structure of $XeF_5^+AsF_6^-$ [5,15] Bartlett and Wechsberg concluded that the former complex was $Xe_2F_{11}^+AsF_6^-$. Although they were able to obtain single crystals of the arsenic complex, all showed disorder or gross twinning features and were unsuitable for an X-ray structure determination. Sladky and Bartlett[5] had similar difficulties in preparing single crystals of $Xe_2F_{11}^+RuF_6^-$, which was considered to be the best platinum-metal-pentafluoride case (because of the lower atomic number of ruthenium) for a structural characterization of the cation.

The controversy concerning the nature of the bonding in XeF_6[65-67] and the role of the "non-bonding" Xe valence electron pair in determining the shape of the molecule gives added interest to the geometry of the

$Xe_2F_{11}^+$ cation. It seemed even at the outset, however (see Ref. 58), that the complex cation would be a symmetrical fluorine bridged $F_5Xe...F...XeF_5$ species and, in particular, a relationship to the crystalline XeF_6 structure[68] was anticipated.

Although the structure determination of an alkali fluoroaurate would have been more satisfactory for the description of the AuF_6^- ion, single crystals of $MAuF_6$ (M = Cs, Rb, K, etc.) have not yet been obtained. Nevertheless, with allowance for the perturbing influence of the unsymmetrical cation, an adequate description of AuF_6^- has been provided by the structure of $Xe_2F_{11}^+AuF_6^-$.

B. Experimental

1. Preparation

$Xe_2F_{11}^+AuF_6^-$ was prepared as previously described in Chapter IV.[41] Crystals were grown by placing $Xe_2F_{11}^+AuF_6^-$ (1.28 mmoles) and XeF_2 (5.91 mmoles) (see Chapter II), in a Monel autoclave bomb. Fluorine gas (70 mmoles) was added by condensing with liquid nitrogen, then the bomb was heated at 400° for 48 hr under a fluorine pressure of 1000 psi. It was then cooled slowly to room temperature overnight and the excess F_2 and XeF_6 were removed under vacuum. The bomb was opened in the Dri Lab. The $Xe_2F_{11}^+AuF_6^-$ lay in the bottom of the bomb as a mass of small yellow-green plates, whose crystal habit was orthorhombic. Crystals were wedged into small quartz capillaries with Pyrex push rods, then sealed as described in Chapter I. Because $Xe_2F_{11}^+AuF_6^-$ is extremely water sensitive, the utmost precautions were taken to exclude water from all apparatus and materials.

2. Crystal Data

$F_{17}AuXe_2$ (mol wt 782.5) is orthorhombic with $\underline{a}$ = 9.115(6), $\underline{b}$ = 8.542(25) and $\underline{c}$ = 15.726(20)Å, $\underline{V}$ = 1224.3Å^3, $\underline{z}$ = 4, $\underline{D_c}$ = 4.24 g cm^{-3}, $\underline{\mu}$ (Mo Kα) = 182 cm^{-1} and F(000) = 1345.72. The rather large estimated standard deviations of the cell constants reflect changes during data collection, presumably as a consequence of some decomposition. A powder photograph of the bulk material was indexed using the single crystal unit cell dimensions. The unit cell volume satisfies Zachariason's criterion[16] for close packed fluoride lattices, since the effective volume per fluorine atom is 18.0Å^3. Single crystal Weissenberg photographs indicated that the space group was either Pnma (#62) or $Pn2_1b$ (#33 in a non-standard setting). The structure was successfully refined in the centrosymmetric group Pnma. Due to the extreme reactivity of the material no attempt was made to obtain an experimental density.

3. X-Ray Measurements

A Picker automatic four-circle diffractometer equipped with a fine focus Mo anode tube (λ Mo Kα_1 = 0.70926Å), and a graphite monochromator was used for data collection. Accurate cell dimensions were obtained from a least-squares refinement of the orientation matrix and of the cell parameters based on the four angle settings (2θ, ω, ψ and ϕ) of 12 high angle ($45 \leqslant 2\theta < 50°$) reflections. Intensity data were collected by the θ-2θ scan technique, at a scan rate of 2°/min. The scan width was 1.4°. Background counts were offset from the scan limits by 0.8°, and each count lasted 4 sec. Three standards were checked every 50 reflections. The temperature during data collection was 24±1°. Because $Xe_2F_{11}^+$ decomposes slowly in X-rays, four crystals were used in the data

collection. All four were flat plates, elongated along the b axis, and each was mounted with the b axis along the ϕ axis of the diffractometer. The crystals had the following dimensions for the h, k and ℓ directions, respectively: #1, 0.255, 0.345, 0.047; #2, 0.282, 0.351, 0.060; #3, 0.204, 0.462, 0.096; #4, 0.231, 0.600, 0.072 mm (the precision of these measurements is probably no better than ±0.005 mm). Each of the crystals was bounded by the six planes of the forms [100], [010] and [001]. The first three crystals provided a complete set of +h, +k, +ℓ and +h, -k, +ℓ data to $2\theta \leq 40°$ (1204 reflections). A crystal was discarded when an ω scan half width of any standard reflection became $\geq 0.25°$. Intensity decay of the standards was no greater than 20.0% in any one crystal. Corrections for decay were made.

Because of the large absorption coefficient (182 cm^{-1}) and the fact that all the crystals were much larger than the optimum size, the data were corrected for absorption using a program developed by P. Coppens, L. Leiserowitz and D. Rabinovich,[69] modified by D. Cahen and J. Ibers,[70,71] and adapted for local use. This method incorporates numerical integration using a Gaussian grid. The data were treated and weights assigned as previously described[18] with the exception that a g factor (used to decrease the weights of large intensities) of zero was used. Scattering factors[19] for neutral gold, xenon and fluorine were used. Values for anomalous dispersion, $\Delta f'$ and $\Delta f''$, were taken from Cromer and Liberman.[21]

4. Structure Refinement

Initially, the structure was solved using the data from Crystal #4 only ($2\theta \leq 40°$). This set of data yielded an averaged set of 633 unique reflections, of which 529 satisfying the condition $I \geq 3\sigma(I)$ were used in the least-squares refinement.

A Patterson function yielded the positions of the two Xe and one Au atoms and refined to $\underline{R} = 0.21$. The Patterson map confirmed the choice of the centric space group since all the Harker sections had either $\underline{y} = 0$ or $\underline{y} = 1/2$. A difference Fourier based on the set of planes generated by the least-squares refinement gave the positions of all of the fluorine atoms. Least-squares refinement incorporating anisotropic temperature factors for all atoms gave a final $\underline{R}$ factor of 0.04, using the data from Crystal #4.

The data obtained from the first three crystals ($+h, +k, +\ell$, $2\theta \leq 50°$) were then scaled and averaged with the set obtained from crystal #4. Of the 1162 total independent data, the 874 which satisfied the condition $I \geq 3\sigma(I)$ were used for the least-squares refinement. A least-squares refinement using the combined data gave $\underline{R} = 4.48\%$, and weighted $\underline{R}_2 = 3.98\%$.

It was noted that the higher angle data ($40° \leq 2\theta \leq 50°$) had large weighted discrepancies, $w(\Delta F)^2$. These data had been measured only once whereas the data below $2\theta = 40°$ were measured at least three times. For multiply measured data, the estimated standard deviation is based

on the larger of either their counting statistics or their scatter, and thus the standard deviations of the high angle data were consequently smaller. To correct this situation a minimum value corresponding to what was observed for the weaker lower angle data was then applied as a lower limit to the standard deviations of the higher angle data. The four sets of data were rescaled. All of the data with $\sin\theta/\lambda \leq 0.15$, (a total of 22 reflections) were arbitrarily deleted because of excessively large discrepancies; this is no doubt due to the inadequacies of the absorption correction. Examination of the data showed no extinction effects.

The final least-squares refinement, with all atoms anisotropic, gave an $\underline{R}$ factor of 0.052 for all 1140 reflections, and 0.036 for the 862 ($I \geq 3\sigma(I)$) nonzero weighted reflections. The weighted $\underline{R}_2$ was 0.025. The standard deviation of an observation of unit weight was 1.36. The largest shift of any parameter, divided by its estimated standard deviation on the last cycle of least-squares was ≤ 0.0012.

A final difference Fourier showed that the largest residual electron density was 1.91 electrons/Å^3 near the gold atom. Table I gives the positional and thermal parameters from the final refinement. Observed structure factors, standard deviations and differences are given in Table II. Table III gives chemically significant distances and angles.

5. Raman Spectra

Raman spectra of several $Xe_2F_{11}^+$ and XeF_5^+ salts were obtained as described in Chapter I. The results are tabulated in Table IV (see also Chapter IV). For a detailed vibrational spectroscopic study of Xe_2F_{11} and XeF_5^+ salts, see Reference 55.

C. Description of the Structure

As may be seen from Fig. 1 and Table III, the structure analysis clearly defines an AuF_6 group and a Xe_2F_{11} group. The latter consists of two similar XeF_5 groups linked by an additional common F atom. All of these groups (AuF_6, Xe_2F_{11} and its XeF_5 components) possess mirror symmetry.

The AuF_6 group is approximately octahedral, with only one Au-F interatomic distance (Au-F8 = 1.90(1)Å) departing significantly from the average value of 1.86(1)Å. The cis F-Au-F angles are close to 90°; the greatest deviation being for F8-Au-F12 = 88.0(5)°.

Each XeF_5 group of the Xe_2F_{11} species approximates to a square-based pyramid, with the xenon atom placed below the base. The F_{ax}-Xe-F_{eq} angles are ≈80° in both XeF_5 groups. On the other hand, each of the groups departs significantly from C_{4v} symmetry and the cis F_{eq}-Xe-F_{eq} angles in each group are not equivalent. The greatest cis angle of each XeF_5 equatorial set is that furthest from the atom (F7) which links the XeF_5 groups to define the Xe_2F_{11} species. Coincidentally, the greatest cis equatorial angles in each XeF_5 group are also associated with the longest Xe-F distances within the group.

Although the interatomic distances Xe1-F7 and Xe2-F7 are sufficiently short [2.21(1) and 2.26(1) respectively] to warrant the identification of an Xe_2F_{11} group, all other inter-group contacts are sufficiently long that they may be classified as van der Waals contacts. The Xe1-F7-Xe2 angle is not quite linear [169.2(2)°]. The F7-Xe distances are not significantly different and indeed the entire Xe_2F_{11} group has essentially C_{2v} symmetry.

The bridging F atom (F7) is not the only F atom of interest in relationship to the XeF_5 groups. It is seen that each Xe atom of each XeF_5 is approached by three other F atoms (of neighboring AuF_6 groups) as well as by F7. Thus Xe1 is associated with F7, F9, F9' and F8 and Xe2 with F7, F9, F9' and F12 [see Fig. 1(c)]. These sets of four F atoms are arranged about the base of the approximately square-pyramidal XeF_5 groups, such that, together with the F atoms of the XeF_5 they form a distorted capped archimedian antiprism arrangement. The arrangement is illustrated for the Xe1 case, in Fig. 2.

D. Discussion

Prior to the structure determination, chemical, vibrational spectroscopic and Mossbauer evidence[41] had indicated the formulation $Xe_2F_{11}^+$ AuF_6^- for the $F_{17}Xe_2Au$ material. The X-ray structure is fully compatible with that formulation.

The geometry of the AuF_6^- ion is defined for the first time in this structure. A low spin $\underline{d}_{\underline{t}_{2g}}^{6}$ Au(V) electron configuration is anticipated to be akin to the configurations of Pt(IV) and Pd(IV) and like them to favor a regular octahedral MF_6 species. Any departures from octahedral symmetry, in this structure, can be rationalized on the basis of possible distorting influences of the $Xe_2F_{11}^+$ cation which is far from octahedral symmetry itself. The average Au-F anion interatomic distance of 1.86(1)Å compares with the average Pt-F distance[42] of 1.89(5)Å for PtF_6^- in $XeF_5^+PtF_6^-$. The greater nuclear charge of Au relative to Pt is anticipated[57] to result in a shorter M-F bond in the Au case.

This structure is at least of as much interest for its cation as for its anion. To a first approximation the complex cation has the form

anticipated for an assembly of two XeF_5^+ ions and a common F^-. Thus the geometry of each XeF_5 component resembles that of XeF_5^+ (see Chapter III) and the coordination of each Xe atom (represented in Fig. 2) closely resembles that for Xe in XeF_5^+.[14b] A comparison of the geometry of the XeF_5 unit in $Xe_2F_{11}^+$ with that of the XeF_5^+ cation in $XeF_5^+RuF_6^-$ is given in Fig. 3. The close approach of F7 to each Xe atom and the departure of the Xe-F-Xe angle from linearity suggest that a measure of covalence should be incorporated into any bonding description. Nevertheless, the ionic model $XeF_5^+F^-XeF_5^+$ accounts for a number of the observed structural features of $Xe_2F_{11}^+$. Previous papers[14b] (see Chapter III) have argued for steric activity of the non-bonding Xe(VI) electron pair in the pseudo-octahedral XeF_5^+ species. One can allow that the close approach of F^- to XeF_5^+ would deflect the non-bonding valence electron pair from from its axial position towards the bisectors of the F3-Xe1-F3' and the F5-Xe2-F5' angles. Increase in the non-bonding pair repulsive interactions with the Xe1-F3 and Xe2-F5 bonds, consequent upon such deflection of the electron pairs, could also account for the lengthening of the Xe1-F3 and Xe2-F5 interatomic distances. Similarly, the deflection of the Xe(VI) "pairs" could account for shortening of the Xe1-F2 and Xe2-F6 distances. In XeF_5^+ the Xe-F equatorial distances are 1.84Å (see Chapter III).

As may be seen from the Raman data given in Table IV, the complex $4XeF_6 \cdot PdF_4$ (Chapter II) contains essentially the same cation as $Xe_2F_{11}^+AuF_6^-$ and may, therefore, be confidently formulated as $[Xe_2F_{11}^+]_2PdF_6^{2-}$. The F bridging of two XeF_5 groups in the $Xe_2F_{11}^+$ cation appears to be characterized by a "bridge stretch" at ~360 cm^{-1}; but, in keeping with the observed structure, the complex cation otherwise behaves vibrationally like two

weakly coupled XeF_5^+ species.

Since crystalline XeF_6 can be described[68] as $XeF_5^+F^-$ (clustered either in tetramers or hexamers) it is not surprising that $Xe_2F_{11}^+$ looks like a fragment of an XeF_6 tetramer or hexamer. The resemblance is closest to the tetramer. In a bonding description of $Xe_2F_{11}^+$ and crystalline XeF_6, XeF_5^+ and F^- are clearly important contributing canonical forms. Perhaps the best description of $Xe_2F_{11}^+$ is as a resonance hybrid of $(XeF_5^+F^-XeF_5^+)$, $(XeF_6XeF_5^+)$ and $(XeF_5^+XeF_6)$ with the first canonical form dominant.

It seems probable that all XeF_6 complexes with fluoride ion acceptors will prove to be either XeF_5^+ or $Xe_2F_{11}^+$ salts. In particular, the $2XeF_6 \cdot MF_5$ and $4XeF_6 \cdot MF_4$ complexes reported by Cady and his co-workers[31,64] are very probably $Xe_2F_{11}^+$ salts.

Table I. Positional and thermal parameters for $Xe_2F_{11}^+AuF_6^-$ with estimated standard deviations in parentheses.

ATOM	X	Y	Z	B11	B22	B33	B12	B13	B23
AU	.15834(6)	.250*	.02276(5)	2.42(3)	3.32(3)	3.95(3)	0*	-.44(2)	0*
XE(1)	.29072(9)	.250*	.66069(7)	2.80(4)	4.73(6)	3.03(5)	0*	.32(3)	0*
XE(2)	.2013(1)	.250*	.38245(7)	3.08(4)	5.06(6)	3.36(5)	0*	-.65(3)	0*
F(1)	.234(1)	.250*	.7726(6)	7.0(5)	7.9(7)	2.3(4)	0*	1.0(4)	0*
F(4)	.077(1)	.250*	.2933(7)	6.5(6)	11.1(8)	5.3(6)	0*	-3.7(4)	0*
F(7)	.2238(8)	.250*	.5254(6)	4.4(4)	4.8(5)	3.7(5)	0*	-.2(4)	0*
F(8)	.041(1)	.250*	-.0771(6)	4.1(4)	8.3(6)	5.4(5)	0*	-1.6(4)	0*
F(10)	.270(1)	.250*	.1212(7)	5.6(5)	7.2(6)	5.9(7)	0*	-3.2(4)	0*
F(11)	.3300(9)	.250*	-.0407(7)	3.1(4)	9.3(8)	6.9(7)	0*	1.0(4)	0*
F(12)	-.0143(9)	.250*	.0857(6)	3.1(4)	9.9(7)	5.5(5)	0*	.6(3)	0*
F(2)	.1448(6)	.1026(9)	.6578(4)	4.3(3)	6.1(4)	5.3(4)	-1.9(3)	1.0(2)	.2(3)
F(3)	.4114(7)	.0949(8)	.7046(4)	5.0(3)	6.3(4)	5.1(4)	1.5(3)	.0(2)	1.3(3)
F(5)	.2914(7)	.096(1)	.3168(5)	5.9(4)	11.3(7)	7.0(5)	1.7(4)	-.0(3)	-4.5(5)
F(6)	.0708(6)	.1013(8)	.4160(5)	3.6(3)	5.4(4)	8.1(5)	-1.4(2)	-.9(2)	.1(3)
F(9)	.1587(8)	.033(1)	.0236(6)	8.2(4)	4.3(4)	9.6(6)	-.2(3)	-3.0(4)	.3(4)

* Fixed Parameter

Table II. Observed structure factors, standard deviations and differences (x 1.0) for $Xe_2F_{11}^{+}AuF_6^{-}$.

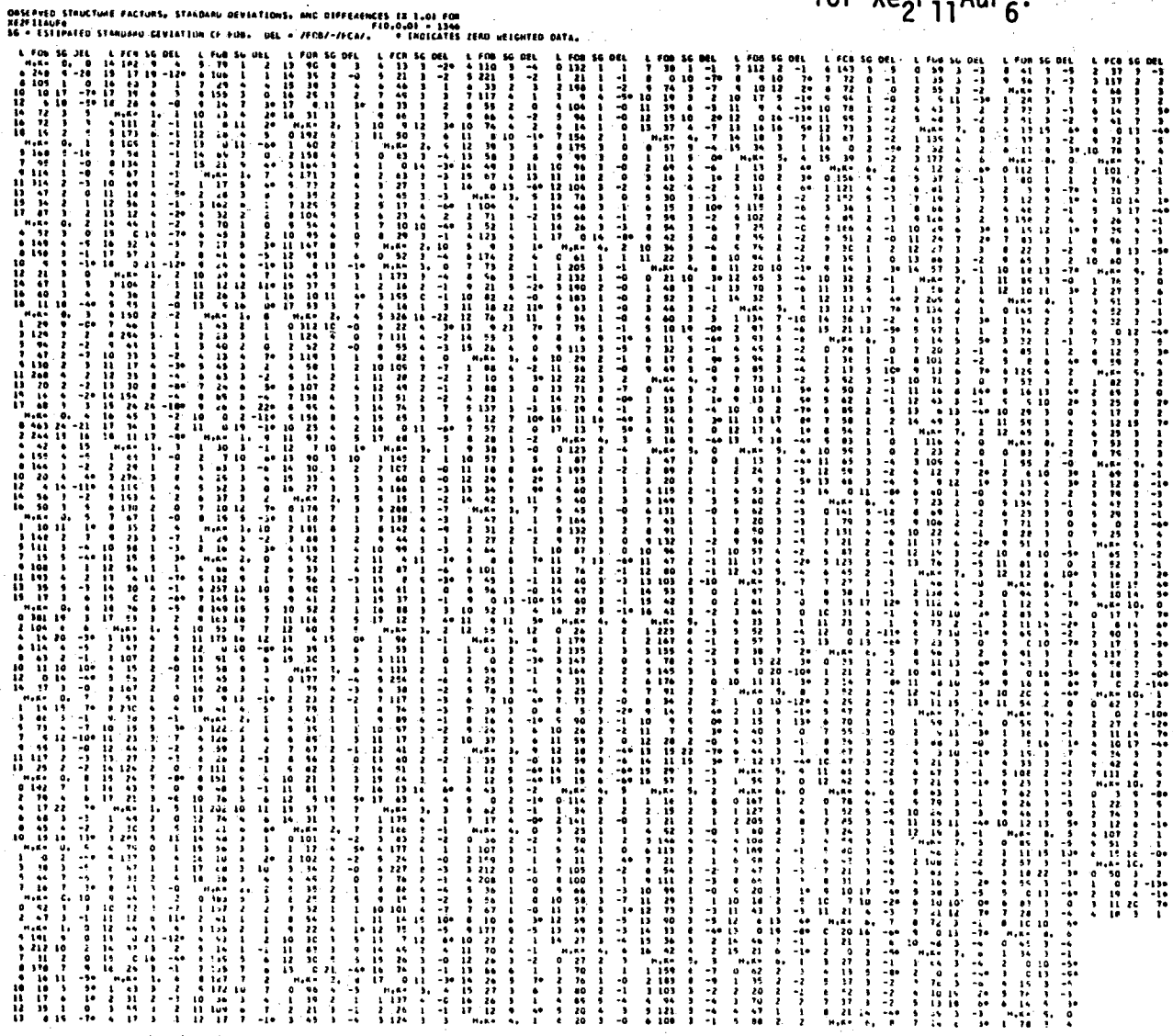

XBL 7210-7128

TABLE III

Interatomic Distances(Å) and Angles(DEG.) for $Xe_2F_{11}^+AuF_6^-$

(Estimated Standard Deviations are in Parentheses)

Anion		Cation			
F9-Au-F9'	179.1(3)°	F1-Xe1-F2	79.6(4)°	F4-Xe2-F6	79.4(4)°
F8	90.4(4)	F3	79.0(4)	F5	81.1(5)
F8-Au-F11	91.6(6)	F2-Xe1-F2	86.8(3)	F6-Xe2-F6	88.6(3)
12	88.0(5)	F3	87.1(4)	F5	87.4(6)
F10-Au-F11	89.2(5)	F3-Xe1-F3	91.1(3)	F5-Xe2-F5	89.9(3)
F12	91.2(6)	Xe2-F7-Xe1	169.2(2)		
Interionic Distances and Angles					
Xe1-F8	2.64(1) Å	F1-Xe1-F7	147.6(6)°	F4-Xe2-F7	146.3(7)°
F9	3.27(1)	F8	136.3(6)	F12	139.8(7)
Xe2-F12	2.64(1)	F9	132.2(3)	F9	135.9(2)
F9	3.52(1)				

TABLE IV

Raman Spectra of $Xe_2F_{11}^+$ Salts and Related Species (shifts in cm^{-1})

IF_5[a]	$(NO^+)_2PdF_6^{2-}$	$(XeF_5^+)_2PdF_6^{2-}$	$(Xe_2F_{11}^+)_2PdF_6^{2-}$	$(Xe_2F_{11}^+)AuF_6^-$	$Cs^+AuF_6^-$
710(ν_1) vs		653 s	668 w 651 vs	661 s	
631(ν_7) sh		634 vw	630 m	640 w	
614(ν_2) vs		616 vw 606 w	615 w 610 m 606 w	626 w 600 s	
602(ν_4) sh		590 ms	591 s 583 m	595 vs 590 vs	595(ν_1) vs
	573(ν_1) s	558 ms	568 s		
	554(ν_2) ms	535 s	546 w		
					530(ν_2) vw
370(ν_8) w		425 vw 396 vw	412 vw 396 vw	400 w	
			375 w	356 w	
318(ν_3) m		309 w	296 w (b)	290 w	
274(ν_6) w		269 w	270 w (b)	---	
	243(ν_5) ms	245 w	245 w (b)		
				221 m	224(ν_5) s

(a) L. E. Alexander and I. R. Beattie, J. Chem. Soc. (A), 1971, 3091.

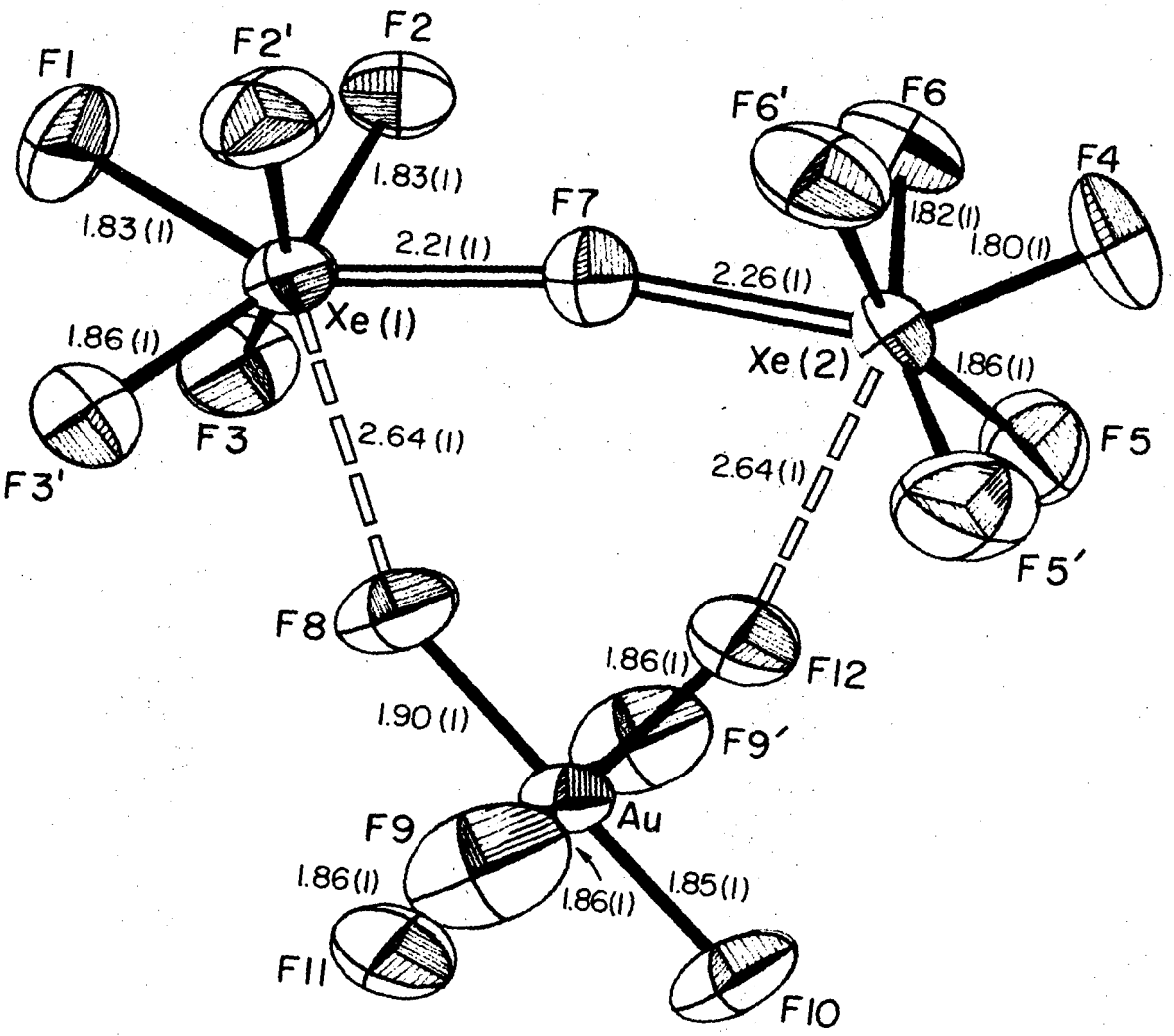

Fig. 1(a). The structural unit $Xe_2F_{11}^+AuF_6^-$.

XBL7210-7119A

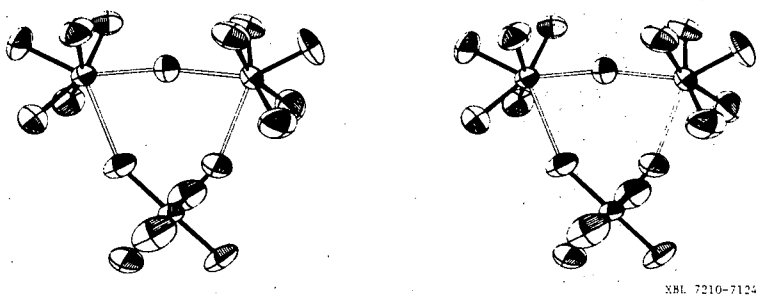

Fig. 1(b). Stereogram of the $Xe_2F_{11}^+AuF_6^-$ structure unit.

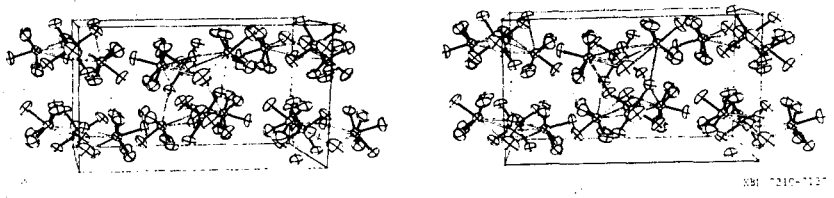

Fig. 1(c). Stereogram showing the arrangement of the $Xe_2F_{11}^+AuF_6^-$ units in the unit cell--view along the b axis.

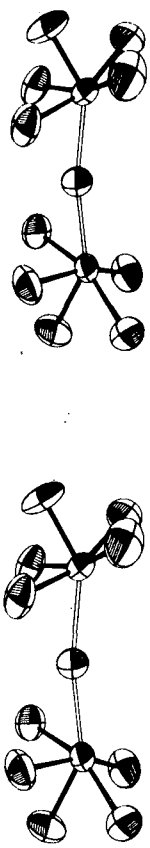

XBL 7210-7129

Fig. 1(d). Stereogram of the $Xe_2F_{11}^+$ ion.

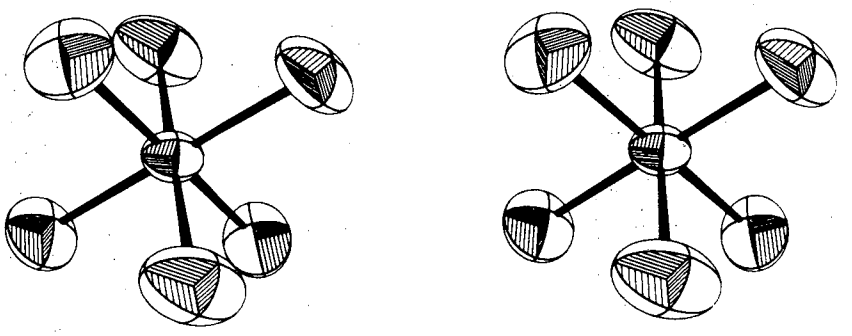

XBL 7210-7130

Fig. 1(e). Stereogram of the AuF_6^- ion.

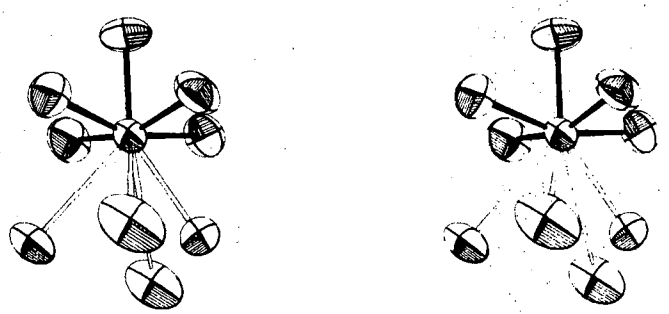

XBL 7210-7125

Fig. 2. Stereogram showing the typical Xe coordination in F atoms (exemplified by Xe(1) coordination).

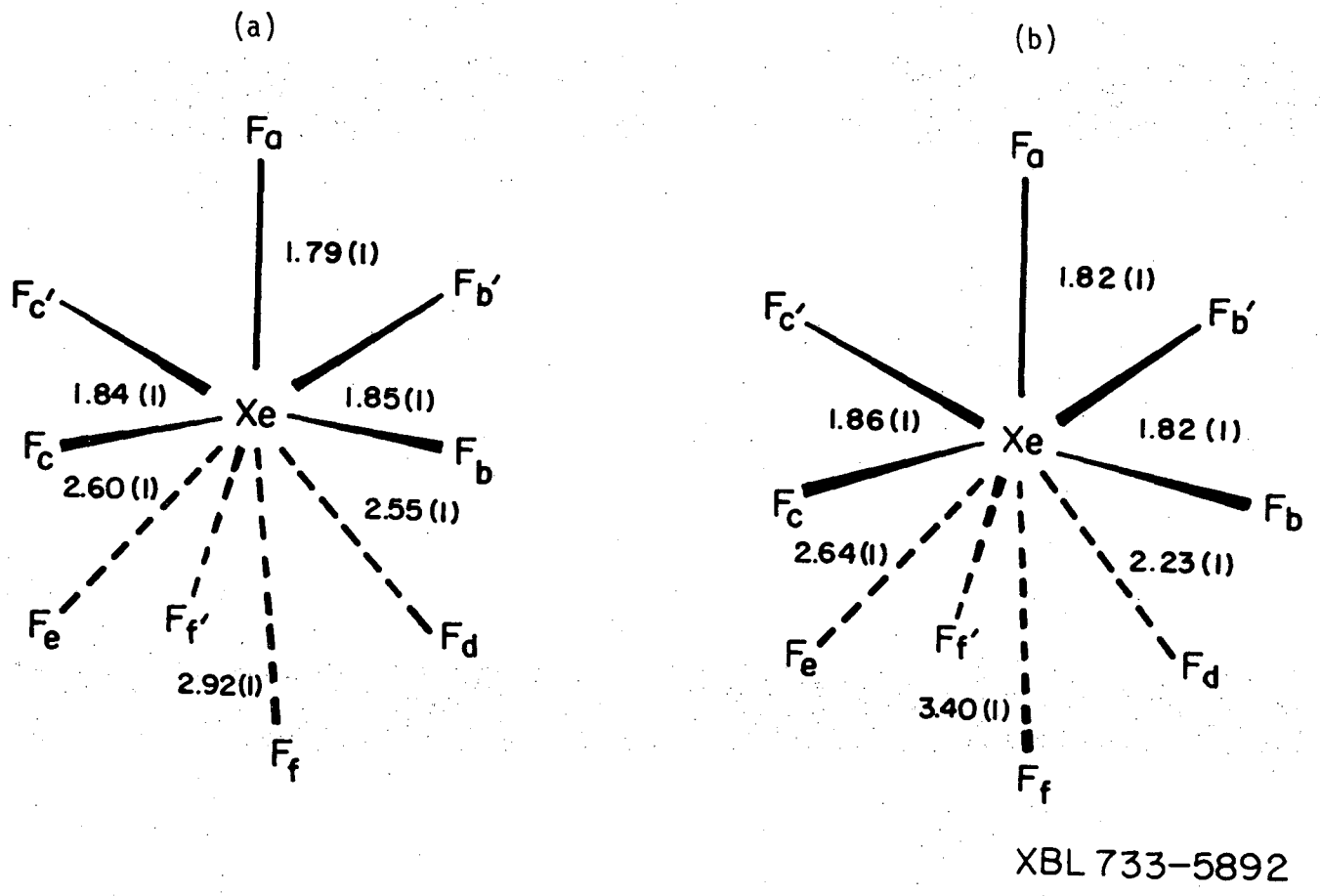

Fig. 3. Comparison of the XeF_5 unit in (a) $XeF_5^+RuF_6^-$ and (b) $Xe_2F_{11}^+AuF_6^-$.

Table for Figure 3

	XeF_5^+ in $XeF_5^+RuF_6^-$ [a]	XeF_5 unit (av.) in $Xe_2F_{11}^+AuF_6^-$
F_{eq}-Xe-F_{ax}	79.0(2)°	79.9(2)°
F_b-Xe-F_b'	87.8(2)	87.7(2)
F_c-Xe-F_c'	87.0(2)	90.5(2)
F_b-Xe-F_c	88.4(4)	87.2(3)
F_d-Xe-F_a	142.3(7)	147.0(5)
F_e-Xe-F_a	140.6(6)	138.0(5)
F_f-Xe-F_a	129.6(3)	134.0(2)

(a) Ref. 14(b)

VI. MÖSSBAUER STUDY OF QUINQUEVALENT GOLD COMPOUNDS

A. Introduction

At the time of the discovery of Gold(V) compounds, Mössbauer spectroscopy offered an additional tool to both confirm the quinquevalent oxidation state of gold in these compounds and support the octahedral form predicted for the AuF_6^- anion. The 77.3 keV $1/2^+ \rightarrow 3/2^+$ M1(12.4% E2) gamma transition of monoisotopic $^{197}Au^{72}$ is well suited for chemical applications of Mössbauer spectroscopy, since the observed ranges of isomer shifts and electric quadrupole splittings amount to several experimental linewidths.

Consequently, Au(III) and Au(I) compounds have been the subject of extensive investigations by nuclear gamma resonance spectroscopy.[73-75] The results revealed a dependence of the isomer shift on the oxidation state similar to that found in compounds of the 3d, 4d and 5d transition elements, e.g., ^{57}Fe, ^{99}Ru, ^{193}Ir and ^{189}Os.[76] On the other hand, appreciable variation of the isomer shift within the same oxidation state was observed for an Au(III) compounds, much as in the cases of Ru(II) and Ru(III);[77,78] Ir(III);[79] and Fe(II)[80] low-spin complexes, indicating a marked dependence of the isomer shift upon the nature of the ligands.

B. Experimental

1. Preparation of Gold Compounds

$Xe_2F_{11}^+AuF_6^-$, $XeF_5^+AuF_6^-$, $Cs^+AuF_6^-$ and AuF_3 were prepared and characterized as described in Chapter IV. Since all of these compounds are extremely water sensitive, the utmost precautions were taken to exclude moisture from all apparatus and materials. Absorber capsules

were loaded in a Vacuum Atmospheres Corporation Drilab (N_2 atm), and were checked after Mössbauer measurements to ensure the sustained quality of the samples.

2. Mössbauer Technique

All samples were put into vacuum-tight, indium-metal-gasketed absorber capsules made of aluminum with inner containers made of Kel-F. The thickness of each absorber was adjusted to approximately 50 mg/cm^2 of ^{197}Au. The standard Mössbauer transmission experiments were performed with both source and absorber cooled to 4.2°K, using a sinusoidal velocity spectrometer[81] and a Ge(Li)-diode for recording the 77.3 keV gamma rays. In the determination of isomer shifts, the channels corresponding to maximum velocity are obtained from symmetry arguments alone.[81] This method gives very precise values for isomer shifts.

Sources of ^{197}Pt, in platinum metal, were prepared by neutron irradiation of platinum metal foils (about 3 mg, enriched to 65% in ^{196}Pt) in an integrated thermal neutron flux of 3×10^{19} n/cm^2. These foils were used as received from the reactor, without further treatment. They were re-irradiated repeatedly.

C. Results and Discussion

Figure 1 shows, as an example, the Mössbauer spectrum of $Xe_2F_{11}^+AuF_6^-$; a single unbroadened resonance line is observed. The solid line is the result of a least-squares fit of a Lorentzian line to the data. Almost identical Mössbauer spectra were obtained for $XeF_5^+AuF_6^-$ and $Cs^+AuF_6^-$. Since the previously reported[73] shift for AuF_3 was very different from the AuF_4^- shifts, and was obtained from a reportedly[73] decomposing sample, the Mössbauer spectrum of AuF_3 was also measured.

Due to electric quadrupole splitting of the $I^{\pi} = 3/2^{+}$ nuclear ground state of ^{197}Au, the resulting Mössbauer spectrum consists of two Lorentzian lines separated by $\Delta E_Q = 2.71 \pm 0.02$ mm/s.

The results are summarized in Table I. The observed experimental linewidths, when corrected for line-broadening caused by finite absorber thickness,[82] compare quite well with twice the natural width of the Mossbauer gamma rays, $W_o = 2\hbar/\tau = 1.85 \pm 0.01$ mm/s.[83] This puts an upper limit of $\Delta E_Q < 0.05$ mm/s to the possible electric quadrupole interaction at the gold sites in these quinquevalent compounds, which is in agreement with the observed octahedral symmetry of the AuF_6^- anion in the crystal structure of $Xe_2F_{11}^+AuF_6^-$ (see Chapter V).

Moreover, structural data also indicate an octahedral anion in both $Cs^+AuF_6^-$ and $XeF_5^+AuF_6^-$. $Cs^+AuF_6^-$ is isomorphous with $Cs^+OsF_6^-$, the structure of which[50] shows the anion to be octahedral. $XeF_5^+AuF_6^-$ is isostructural with $XeF_5^+AsF_6^-$ (Chapter IV), the anion of which[15] is nearly octahedral.

The results for the isomer shift $\underline{S}$ of the quinquevalent compounds, listed in column 4 of Table I, are almost identical with each other, supporting the existence of similar AuF_6^- anions in all of the studied quinquevalent gold compounds. This has also been concluded from the close similarity of the Raman spectra obtained for these complexes (Chapter IV, V). The results for isomer shift and electric quadrupole splitting found for AuF_3 agree well with those given in Ref. 73.

A graphical representation of the present isomer shift results, together with those for Au(III) and Au(I) compounds with halogen ligands, taken from Refs. 73-75 is presented in Fig. 2. With the exception of AuF_3, the isomer shifts arrange themselves in three well separated groups

corresponding to univalent, tervalent and quinquevalent gold. As in the case of compounds of Fe, Ru, Ir, Pt and Os.[76-80,84,85] The isomer shifts exhibit a monotonic dependence on the oxidation state.

Assuming constant electron density within the nucleus, one can write for the isomer shift $\underline{\underline{S}}$ in velocity units[86]

$$\underline{\underline{S}} = c/E_\gamma \cdot 2\pi/3 \cdot Z \cdot e^2 \cdot \Delta\langle r^2\rangle \cdot \Delta\rho(0)$$

where $\Delta\langle r^2\rangle = \langle r^2\rangle_e - \langle r^2\rangle_g$ is the change of the mean-squared nuclear charge radius between the excited state and the ground state of the nucleus, and $\Delta\rho(0)$ stands for the difference of the total electron density at the Mössbauer mucleus in the two chemical environments. E_γ is the energy of the Mössbauer gamma rays and c, e and Z have their usual meanings.

The total electron density at the nucleus $\rho(0)$ depends on the nature of the chemical bonding. Positive contributions to $\rho(0)$ arise from the atomic 6$\underline{s}$ populations of the molecular orbitals on the gold ion, while a decrease in $\rho(0)$ is caused by the atomic 5$\underline{d}$ populations due to their shielding effects on $\underline{s}$ electrons. The relative magnitudes of the various contributions are known from the results of relativistic free-ion self-consistent field calculations for gold[87] and for other $\underline{d}$ transition elements. The atomic 6$\underline{p}$ populations, on the other hand, yield only small contributions both by shielding of $\underline{s}$ electrons and by their relativistic density at the nucleus.[87] Hence $\rho(0)$ and consequently the isomer shift will mainly depend on the atomic 6$\underline{s}$ and 5$\underline{d}$ populations on the gold ion.

From the effects of quasi-hydrostatic pressure on the transition energy of the 77.3 keV gamma rays of ^{197}Au in metallic gold, a value of $\Delta\langle r^2\rangle \simeq +9\times10^{-3}$ fm^2 has been derived for the change of the mean-squared nuclear charge radius.[88] The positive sign of $\Delta\langle r^2\rangle$ implies an increase in $\rho(0)$ with increasing isomer shift. The isomer shift results of Fig. 2 thus reveal an increase in $\rho(0)$ with increasing oxidation state of gold. This is what is expected on the basis of d electron shielding arguments, assuming a decrease in the atomic population of 5d orbitals on gold going from univalent to tervalent to quinquevalent gold compounds with halogen ligands. The isomer shifts obtained for the AuF_6^- complexes, therefore, strongly support the assigned quinquevalent oxidation state of gold.

A more quantitative discussion of the isomer shift results of Fig. 2, especially their use for a derivation of an estimate for $\Delta\langle r^2\rangle$, is not straightforward since there are considerable variations in the Au atom coordination in these gold compounds. Au(I) compounds usually contain linear ligand-gold-ligand units in the first coordination sphere,[89] while most of the Au(III) complexes have square-planar molecular symmetry.[90] The Au(V) complexes studied in the present work, on the other hand, have octahedral symmetry (Chapter IV, V).

Bartlett has previously argued[57] for the F ligands in the transition metal hexafluorides being good π-electron donors. If this is the general situation for F attached to a transition metal atom, one can expect the electron population of d_π symmetry atomic orbitals on gold to increase with increasing coordination in F. This effect would offset to some extent d electron density decrease which is coupled with the

oxidation state increase. Thus the isomer shift differences between the various Au oxidation states, involving the same ligand, are smaller than those expected from the s-electron density results of free-ion Dirac-Fock calculations (using the above value for $\Delta\langle r^2\rangle$,[83] for different d-configurations of gold.[88]

It is probable that the greater isomer shift of AuX_4^- (X = Cl, Br, I) relative to AuF_4^- is due to the poor π donor ability of Cl, Br and I relative to F. Alternatively, the availability of d orbitals of the valence-shell quantum number in Cl, Br and I is often cited[91] in arguing for π acceptor properties for these atoms. F atoms, in contrast, do not have this facility.

As may be seen from Fig. 2 the isomer shift for AuF_3 is anomalously low. The observation is firm, the results from a high quality sample being in good agreement with the previous findings.[75] It may be that the low isomer shift of AuF_3 is linked to its structure. The Au atom in AuF_3 is bonded to four F atoms in a planar, roughly square arrangement.[63] The arrangement has C_{2v} symmetry and each $[AuF_4]$ group has two sets of adjacent (cis) Au-F distances: one short at 1.91(4)Å and one long, at 2.04(3)Å. In addition, the gold atom is coordinated to two other F atoms at 2.69(4)Å on an axis roughly perpendicular to the plane defined by the $[AuF_4]$ group. Thus the coordination of the Au atom in AuF_3 may be described approximately as tetragonally-elongated octahedral. In no other Au(III) compound, shown in Fig. 2, is this structure type observed. It is usual for the Au(III) compound to be square or nearly-square coordinated[92] but other ligands approaching the $[AuL_4]$ group always do so well of the axis normal to this plane. The usual situation is

illustrated by the crystal structure of $KAuF_4$.[52]

The AuF_4^- ion in $KAuF_4$ is recognized as the square planar AuF_4 group characterized by an Au-F distance of 1.95(2)Å. (This Au-F distance is not significantly different from the mean of the Au-F distances of the AuF_4 group in AuF_3, which is 1.98(4)Å.) The gold atom in $KAuF_4$ is also coordinated by four other F atoms at 3.12(2)Å. The entire arrangement of eight F atoms about the Au atom can be described as a distorted cubic group. The square AuF_4^- species represents a pair of diagonally opposite parallel edges of the "cube" (which has, in consequence, been distorted to render these edges, and the relating face diagonals, equal). The other two diagonally-opposite parallel edges of the original four-fold cubic set each represent two of the F atoms at 3.12Å from the Au atom.

The coordination of the AuL_4 group in AuF_3 (in contrast to all of the other Au(III) compounds) by two other ligands approximately normal to the AuL_4 plane may account for the anomalously low isomer shift of AuF_3. In the square AuF_4 group of AuF_3, each of the additional F ligands is suitably located for π donation to the Au(III) atom. Thus if the pseudo-four-fold axis of the AuF_4 group is $\underline{z}$, the $\underline{d_{zx}}$ and $\underline{d_{zy}}$ orbital electrons of the Au(III) are more concentrated on that atom than otherwise, as a consequence of the π donor ability of those two F ligands which are nearby on the $\underline{z}$ axis.

For a rough estimate of $\Delta\langle r^2\rangle$ take the isomer shift difference between the AuF_6^- complexes and AuF_3, ΔS = 3.4 mm/s, as representative for the one between Au(V) and Au(III). It is obvious from the above discussion that for this pair of gold compounds the difference in

effective coordination number is smaller than for any other pair of the studied gold compounds with different oxidation states. For the electron density difference between $5\underline{d}^6$ and $5\underline{d}^8$ configurations a value of $\Delta\rho(0) = 4.4\times10^{26}$ cm^{-3}, as estimated from the results of relativistic Dirac-Fock calculations of Ref. 22 for free-ion configurations for gold is taken. One then obtains a value of $\Delta\langle r^2\rangle \simeq 8.6\times10^{-3}$ fm^2 for the change of the mean-squared nuclear charge radius. Because of the change in molecular structure from AuF_6^- to AuF_3, however, this value should be considered as a lower limit for $\Delta\langle r^2\rangle$. It is interesting that it agrees quite well with a result of Ref. 88.

TABLE I

Compilation of experimental results: ε = resonance effect, W = total experimental linewidth (FWHM); S = isomer shift relative to the platinum metal source; $E_Q = e^2 \cdot q \cdot Q(3/2)/2 \cdot (1 + \eta^2/3)^{1/2}$ = electric quadrupole splitting of the nuclear ground state of ^{197}Au.

Compound	ε (%)	W (mm/s)	S (mm/s)	E_Q (mm/s)
$Xe_2F_{11}AuF_6$	2.9	1.98 ± 0.02	2.28 ± 0.01	---
XeF_5AuF_6	4.0	2.10 ± 0.06	2.31 ± 0.02	---
$CsAuF_6$	2.8	2.02 ± 0.06	2.39 ± 0.02	---
AuF_3	4.6	2.00 ± 0.02	-1.06 ± 0.02	2.71 ± 0.02

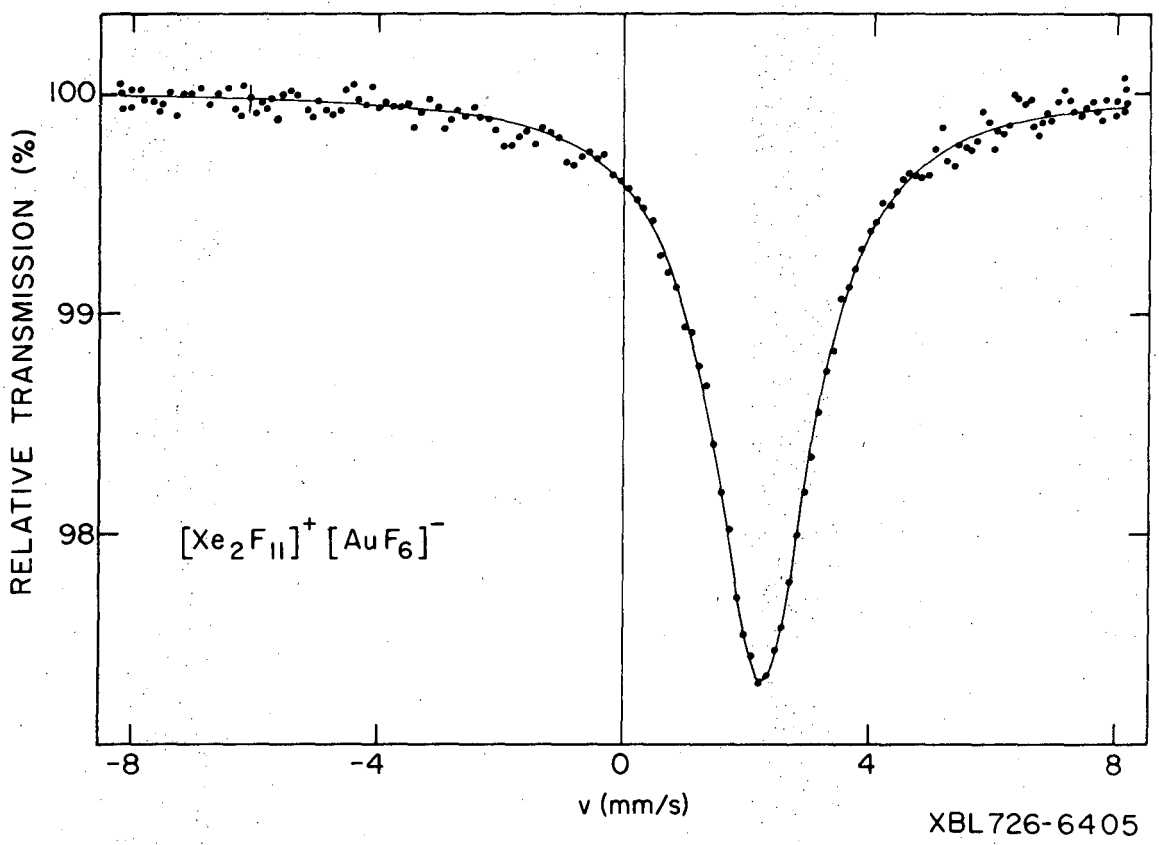

Fig. 1. Mössbauer absorption spectrum of $Xe_2F_{11}^+AuF_6^-$, recorded with the 77.3 keV gamma rays of ^{197}Au, emitted from a metallic ^{197}Pt source. Both source and absorber were at 4.2°K. The solid line is the result of a least-squares fit of a Lorentzian line to the data.

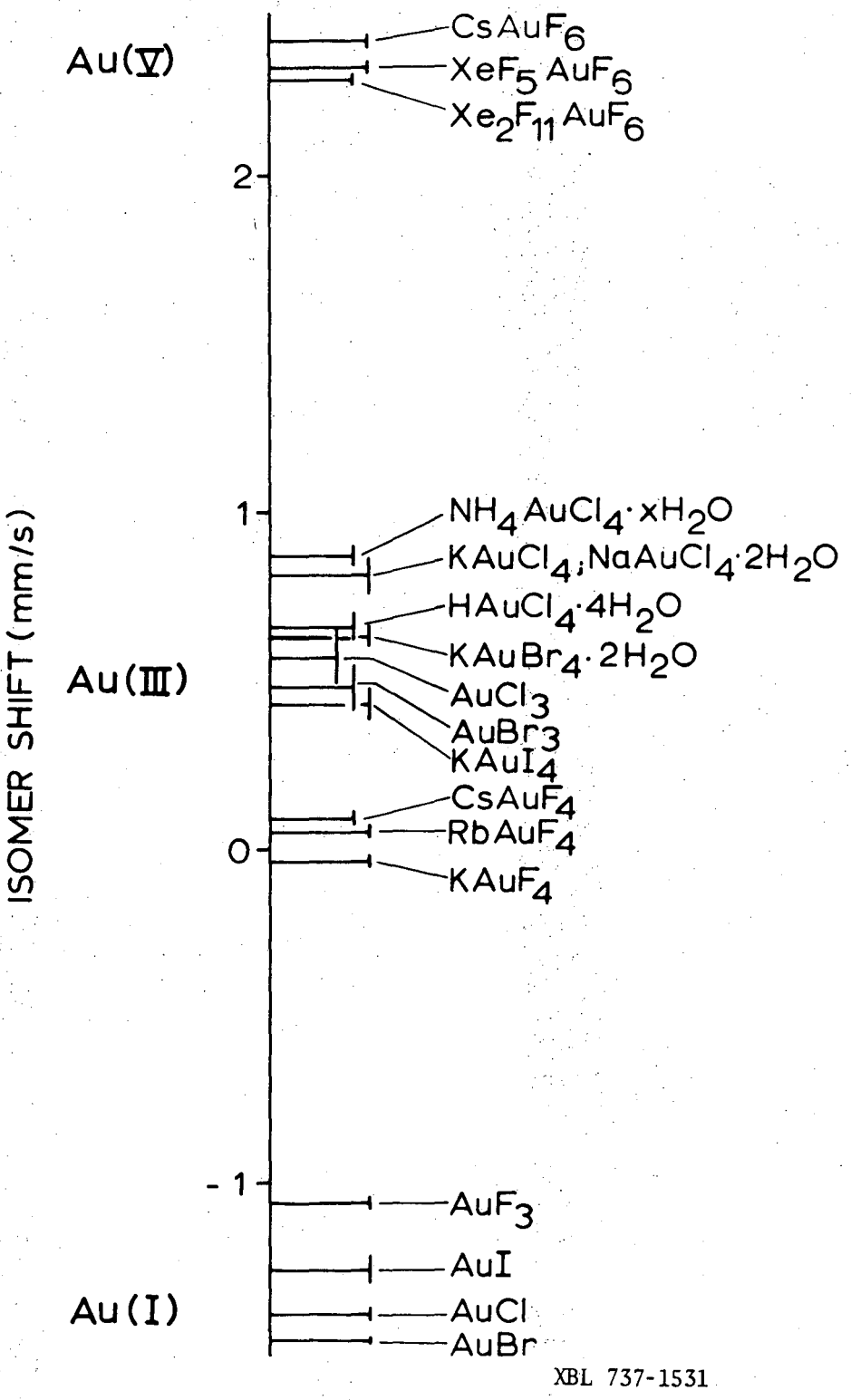

Fig. 2. Graphical representation of isomer shifts of the 77.3 keV gamma rays of ^{197}Au for univalent, tervalent and quinquevalent gold compounds with halogen ligands.

ACKNOWLEDGEMENTS

Special thanks go to Professor Neil Bartlett, who showed me what it means to be a scientist: the joys, the disappointments and the hard work. His infectious enthusiasm, incredible ability, freshness of approach, integrity and good humor made working for him an experience to be treasured.

Thanks also go to Dr. Jim Scherer of USDA, Albany, CA, for generous use of the Raman spectrometer; to Dr. Allan Zalkin of Nuclear Chemistry who was instrumental in solving several difficult crystallographic problems; to Dr. Gunter Kaindl, also of Nuclear Chemistry, for assistance with the Mössbauer experiments.

Andy Anderson, Carl Baugh, Wilton Berlund, Phil Eggers, Walt Toutolmin, Hoy Wong and Howard Wood provided invaluable assistance in the maintenance, design and fabrication of equipment. They also taught me an appreciation for fine tools, excellent work and good company.

Thanks to Jean Wolslegel, Technical Typing Division, for friendly help in getting this thesis typed and filed on schedule.

Special thanks also go to Dr. Dough McKee--his friendship and good humor made even bad days bearable.

Finally, thanks to all my friends, who made the last four years both a personal and professional adventure--it was a good time.

This work was done under the auspices of the U. S. Energy Research and Development Administration.

REFERENCES

1. D. F. Shriver, The Manipulation of Air-Sensitive Compounds (McGraw-Hill, New York, 1969).
2. N. Bartlett and P. R. Rao, Proc. Chem. Soc. 393 (1964).
3. N. Bartlett and J. W. Quail, J. Chem. Soc. 3728 (1961).
4. C. C. Addison and B. G. Ward, Chem. Comm. 6, 155 (1966).
5. F. O. Sladky and N. Bartlett, J. Amer. Chem. Soc. 90, 5316 (1968).
6. N. Bartlett and F. O. Sladky, The Chemistry of Krypton, Radon and Xenon in Comprehensive Inorganic Chemistry, A. F. Trotman-Dickenson, ed. (Pergamon Press, New York, 1974), Vol. 1, p. 299.
7. L. V. Streng and A. G. Streng, Inorg. Chem. 4, 1370 (1965).
8. J. H. Holloway, Chem. Comm. 1, 22 (1966).
9. S. M. Williamson, Inorg. Synthe. 9, 147
10. I. Sheft, T. M. Spittler and F. H. Marten, Science 145, 701 (1964).
11. A. G. Sharpe, J. Chem. Soc. 3444 (1950).
12. N. Bartlett and B. Zemva, to be published.
13. W. E. Falconer, Bell Telephone Laboratories, personal communication to N. Bartlett.
14. (a) N. Bartlett, F. Einstein, D. F. Stewart and J. Trotter, J. Chem. Soc. (A) 1190 (1967).
    (b) N. Bartlett, M. Gennis, D. D. Gibler, B. K. Morrell and A. Zalkin, Inorg. Chem. 12, 1717 (1973).
15. N. Bartlett, B. DeBoer, F. Hollander, F. O. Sladky, D. Templeton and A. Zalkin, Inorg. Chem. 13, 780 (1974).
16. W. H. Zachariasen, J. Amer. Chem. Soc. 70, 2147 (1948).

17. International Tables for X-Ray Crystallography (Kynoch Press, Birmingham, England, 1952), Vol. I.

18. D. D. Gibler, C. J. Adams, M. Fischer, A. Zalkin and N. Bartlett, Inorg. Chem. 11, 2325 (1972).

19. P. A. Doyle and P. S. Turner, Acta Cryst. A24, 390 (1968).

20. D. T. Cromer and J. T. Waber, Acta Cryst. 18, 104 (1965).

21. D. T. Cromer and D. Liberman, J. Chem. Phys. 53, 1891 (1970).

22. All calculations were done on a CDC-6600 computer, using unpublished versions of least-squares, FORDAP and other programs written and revised by A. Zalkin. All drawings were done using ORTEP, C. K. Johnson, Oak Ridge National Laboratory, June 1965.

23. This discussion by D. H. Templeton is taken from K. Leary, D. H. Templeton, A. Zalkin and N. Bartlett, Inorg. Chem. 12, 1726 (1973).

24. A. Zalkin, J. D. Forrester and D. H. Templeton, Inorg. Chem. 3, 1417 (1964).

25. T. Ueki, A. Zalkin and D. H. Templeton, Acta Cryst. 20, 836 (1966).

26. D. W. J. Cruickshank and W. S. McDonald, Acta Cryst. 23, 9 (1967).

27. R. Hoppe and W. Kelmm, Z. Anorg. Chem. 268, 364 (1952).
A. G. Sharpe, J. Chem. Soc. 197 (1953).

28. D. P. Mellor and N. C. Stephenson, Austral. J. Sci. Res. 4A, 407 (1951).

29. R. D. Burbank and G. R. Jones, Science 168, 248 (1970).

30. G. R. Jones, R. D. Burbank and N. Bartlett, Inorg. Chem. 9, 2264 (1970).

31. K. E. Pullen and G. H. Cady, Inorg. Chem. 5, 2077 (1966).
K. E. Pullen and G. H. Cady, Inorg. Chem. 6, 1300 (1967).
K. E. Pullen and G. H. Cady, Inorg. Chem. 6, 2267 (1967).

32. N. Bartlett and D. H. Lohmann, Proc. Chem. Soc. 115 (1962).
N. Bartlett, Proc. Chem. Soc. 218 (1962).

33. N. Bartlett, S. P. Beaton and N. K. Jha, Chem. Comm. 168 (1966).

34. P. Barberi and N. Bartlett, to be published.

35. N. Bartlett and P. R. Rao, Abstracts of papers, 154th Meeting of the ACS, 1967, K15.
P. R. Rao, Ph. D. Thesis, Univ. of British Columbia, 1965.

36. J. R. Morton and H. W. Wilcox, Inorg. Synth. IV, 48

37. A. A. Woolf, J. Chem. Soc. 619 (1964).

38. K. O. Christe and W. Sawodny, Inorg. Chem. 12, 2879 (1973).

39. A. G. Sharpe, J. Chem. Soc. 2901 (1949).

40. A. A. Woolf, J. Chem. Soc. 1053 (1950).

41. K. Leary and N. Bartlett, Chem. Comm. 903 (1972).

42. N. Bartlett, F. W. B. Einstein, D. F. Stewart and J. Trotter, Chem. Comm. 550 (1966).

43. (a) K. Leary, A. Zalkin and N. Bartlett, Chem. Comm. 131 (1973).
(b) K. Leary, A. Zalkin and N. Bartlett, Inorg. Chem. 13, 775 (1974).

44. N. Bartlett and C. J. Adams, unpublished observation, see also K. Leary and N. Bartlett, Abstracts 7th Intern. Fluorine Symp. (Santa Cruz, 1973), paper I-32.

45. D. Babel, Structure and Bonding 3, 11 (1967).

46. N. Bartlett and D. H. Lohmann, J. Chem. Soc. 5253 (1962).

47. T. J. Richardson, Ph. D. Thesis, Univ. of California, 1974.

48. S. P. Beaton, Ph. D. Thesis, Univ. of British Columbia, 1963.

49. J. H. Canterford and R. Colton, Halides of the Second and Third Row Transition Metals (Wiley-Interscience, New York, 1968).

50. M. A. Hepworth, K. H. Jack, G. J. Westland, J. Inorg. and Nucl. Chem 2, 79 (1956).

51. G. Kaindl, K. Leary and N. Bartlett, J. Chem. Phys. 59, 5050 (1973).

52. A. J. Edwards and G. R. Jones, J. Chem. Soc. (A) 13, 1936 (1969).

53. K. Nakamoto, Infrared Spectra of Inorganic and Coordination Compounds (Wiley-Interscience, New York, 1970), 2nd Edition.

54. I. Wharf and D. F. Shriver, Inorg. Chem. 8, 914 (1969).

55. N. Bartlett and C. J. Adams, Tautomerism in Xenon Hexafluoride: An Investigation of XeF_6 and Its Complexes, submitted to Inorg. Chem.

56. F. O. Sladky, P. A. Bulliner and N. Bartlett, J. Chem. Soc. (A) 2179 (1969).

57. N. Bartlett, Angewandte Chemie Int. Ed 7, 433 (1968).

58. N. Bartlett and M. Wechsberg, Z. Anorg. Chem. 385, 5 (1971).

59. D. E. McKee, C. J. Adams, A. Zalkin and N. Bartlett, J. Chem. Soc. Chem. Comm 26 (1973).

60. A. J. Edwards, Chem. Comm. 820 (1970).

61. A. J. Edwards, W. E. Falconer, J. E. Griffiths, W. A. Sander and M. J. Vasile, J. Chem. Soc. (Dalton) 11, 1129 (1974).

62. W. E. Falconer, personal communication to N. Bartlett.

63. N. Bartlett, F. Einstein, D. Stewart and J. Trotter, J. Chem. Soc. (A) 478 (1967).

64. G. L. Gard and G. H. Cady, Inorg. Chem. 3, 1945 (1964).

65. L. S. Bartell, R. M. Gavin, Jr., H. B. Thompson and C. L. Chernick, J. Chem. Phys. 48, 2547 (1965); K. Hedberg, S. H. Peterson, R. R. Ryan and B. Weinstock, J. Chem. Phys. 44, 1726 (1966); R. M. Gavin, Jr. and L. S. Bartell, J. Chem. Phys. 48, 2460 (1968);

and L. S. Bartell and R. M. Gavin, Jr., J. Chem. Phys. 48, 2466 (1968).

66. R. F. Code, W. E. Falconer, W. Klemperer and I. Ozier, J. Chem. Phys. 47, 4955 (1967).
W. E. Falconer, A. Büchler, J. L. Stauffer and W. Klemperer, J. Chem. Phys. 48, 312 (1968).

67. G. L. Goodman, J. Chem. Phys. 56, 5038 (1972).

68. R. D. Burbank and G. R. Jones, Science 168, 248 (1970).

69. P. Coppens, L. Leiserowitz and D. Rabinovich, Acta Cryst. 18, 1035 (1965).

70. J. A. Ibers and D. Cahen, private communication to A. Zalkin.

71. D. Cahen and J. A. Ibers, J. Appl. Cryst. 5, 398 (1972).

72. A. H. Muir, K. J. Ando and H. M. Coogan, Mössbauer Effect Data Index 1958-1965 (Interscience Publishers, N. Y., 1966).

73. M. O. Faltens and D. A. Shirley, J. Chem. Phys. 53, 4249 (1970).

74. H. D. Bartunik, W. Potzel, R. L. Mössbauer and G. Kaindl, Z. Physik 240, 1 (1970).

75. J. S. Charlton and D. I. Nichols, J. Chem. Soc (A) 1484 (1970).

76. G. Kaindl, D. Kucheida, W. Potzel, F. E. Wagner, U. Zahn and R. L. Mössbauer in Hyperfine Interactions in Excited Nuclei, G. Goldring and R. Kolish, eds (Gordon and Breach, New York, 1971), p. 595 and references therein.

77. G. Kaindl, W. Potzel, F. E. Wagner, U. Zahn and R. L. Mössbauer Z. Physik, 226, 103 (1969).

78. W. Potzel, F. E. Wagner, U. Zahn, R. L. Mössbauer and J. Danon, Z. Physik 240, 306 (1970).

79. F. E. Wagner and U. Zahn, Z. Physik 233, 1 (1970).

80. G. M. Bancroft, M. J. Mays and B. E. Prater, J. Chem. Soc. (A) 956 (1970).

81. G. Kaindl, M. R. Maier, H. Schaller and F. Wagner, Nucl. Instr. Math. 66, 277 (1968).

82. J. Heberle and S. Franco, Bull, Am. Phys. Soc. 13, 60 (1968).

83. D. J. Erickson, L. D. Roberts, J. W. Burton and J. O. Thomson, Phys. Rev. B3, 2180 (1971).

84. F. E. Wagner, D. Kucheida, U. Zahn and G. Kaindl, Z. Physik, in press.

85. D. Walcher, Z. Physik 246, 123 (1971).

86. D. A. Shirley, Rev. Mod. Phys. 36, 339 (1964).

87. J. B. Mann, Los Alamos Scientific Laboratory, personal communication to G. Kaindl.

88. L. D. Roberts, D. O. Patterson, J. O. Thomson and R. P. Levey, Phys. Rev. 179, 656 (1969).

89. H. Jagodzinski, Z. Krist. 112, 80 (1959).

90. M. Bonamico, G. Dessy and A. Vaciago, Anti Occad. Nazl. Lincei. Rend., Classe Sci. Fis. Mat. Nat. 39, 504 (1965).

91. F. A. Cotton and G. Wilkinson, Advanced Inorganic Chemistry (Wiley Interscience, 1966), 2nd Edition, p. 379.

92. E. S. Clark, D. H. Templeton, C. H. MacGillavry, Acta Cryst. 11, 284 (1958).

TECHNICAL INFORMATION DIVISION
LAWRENCE BERKELEY LABORATORY
UNIVERSITY OF CALIFORNIA
BERKELEY, CALIFORNIA 94720